

STUDY OF THUMB ATTITUDE RELATIONSHIP TO  
EXTRINSIC MUSCLES CHARACTERIZATION

BY

MUHAMMAD MUKHLIS BIN SUHAIMI

A thesis submitted in fulfilment of the requirement for the  
Master of Science Engineering.

Kulliyyah of Engineering  
International Islamic University Malaysia

MARCH 2023

## ABSTRACT

In the case of amputees, the development of cybernetic hands that closely resemble the functions of real hands is essential for comfort and functionality purposes. Controlled by intrinsic and extrinsic muscles, the human thumb plays a major role in differentiating hand gestures. For those who have lost their intrinsic hand muscles, any information about muscle activities that can be obtained from the extrinsic muscles is essential to control the thumb. Thus, focusing on transradial amputees, this research investigates the relationship between extrinsic muscles to characterise thumb posture. A High-Density surface Electromyogram (HD-sEMG) device and a portable thumb force measurement system were used to collect forearm HD-sEMG signals from a total of 17 subjects. For the flexion motion, the subjects were asked to repetitively place their thumb at rest before exerting 30% of their individual maximum voluntary contraction (MVC) on a load cell by following a designated trajectory presented on a developed graphical user interface (GUI). The measurement system was set to four different postures namely zero degrees, thirty degrees, sixty degrees, and ninety degrees. Feature extraction was then performed by extracting the absolute rectified value (ARV), root mean square (RMS), mean frequency (MNF) and median frequency (MDF) values of the forearm HD-sEMG signals before being classified using four different classifiers namely linear discriminant analysis (LDA), support vector machine (SVM), k-Nearest Neighbour (KNN), and TREE-based classifier. The results revealed that the LDA classified RMS and ARV-RMS features, which were extracted from both posterior and anterior hand sides successfully achieved the highest correctly classified percentage of 99.7%. The findings of the study are significant for the development of a dedicated model-based control framework for prosthesis hand development to be used by transradial amputees in the near future.

## ملخص البحث

بالنسبة للأشخاص المبتورين، تطوير اليد الإلكترونية التي تشبه اليد الحقيقية في العمل أمر مهم للراحة والأداء الوظيفي. إن العضلات الداخلية والخارجية تتحكم بالإبهام ، فيلعب الإبهام دوراً رئيسياً في إنتاج حركات اليد المختلفة. بالنسبة لأولئك الذين فقدوا عضلات يدهم الداخلية ، فأبي معلومات حول أنشطة العضلات التي يمكن الحصول عليها من العضلات الخارجية ستكون ضرورية للتحكم في الإبهام. يركز هذا البحث على مبتوري المرفق ، فيبحث هذا البحث في العلاقات بين العضلات الخارجية لتصوير وضعية الإبهام الحقيقية. قد استُخدمَ جهازُ تسجيل مخطط كهربية العضل السطحي عالي الكثافة أو ما يعرف أيضاً ب (HD-sEMG) ونظامٌ قياس قوة الإبهام المحمول لجمع إشارات تخطيط كهربائي العضل (EMG) من إجمالي 17 شخصاً. بالنسبة لحركة الانثناء ، طُلب من المشاركين وضع إبهامهم في حالة الراحة بشكل متكرر قبل ممارسة 30 ٪ من الحد الأقصى للانكماش الطوعي (MVC) الفردي على خلية تحميل باتباع مسار معين معروض على واجهة مستخدم رسومية (GUI) معينة. تم ضبط المسار على أربعة أوضاع مختلفة وهي درجة الصفر ، وثلاثين درجة ، وستين درجة ، وتسعين درجة. ثم تم استخراج البيانات عن طريق استخراج المطلقة القيمة المقومة (ARV)، وجذر متوسط مربع (RMS)، قيمة متوسط التردد (MNF) وقيم التردد المتوسط (MDF) لإشارات الساعدِ HD-sEMG قبل تصنيفها باستخدام أربعة مصنفات مختلفة وهي التحليل التمييزي الخطي (LDA) ، وشعاع الدعم الآلي (SVM) ، وكبي أقرب جار (KNN) والمصنف المستند إلى (TREE based classifier) TREE. أظهرت النتائج أن بيانات RMS و ARV-RMS لمصنفة LDA التي نستخرجها من HD-sEMG من كلا الجانبين الخلفي والأمامي لليد قد حققت بنجاح أعلى نسبة مصنفة بشكل صحيح بنسبة 99.7٪. تعتبر نتائج البحث مهمة لتطوير إطار تحكم قائم على النموذج لتطوير اليد الاصطناعية يستخدمه مبتوري المرفق في المستقبل.

## APPROVAL PAGE

I certify that I have supervised and read this study and that in my opinion, it conforms to acceptable standards of scholarly presentation and is fully adequate, in scope and quality, as a dissertation for the degree of Master of Science (Mechatronic Engineering).



.....  
Aimi Shazwani Ghazali  
Supervisor



.....  
Ahmad Jazlan Haja Mohideen  
Co-Supervisor



.....  
Shahrul Na'im Bin Sidek  
Co-Supervisor

I certify that I have read this study and that in my opinion it conforms to acceptable standards of scholarly presentation and is fully adequate, in scope and quality, as a dissertation for the degree of Master of Science (Mechatronic Engineering).

.....  
Muhammad Ibn Ibrahimy  
Internal Examiner

.....  
Wan Khairunizam B. Wan Ahmad  
External Examiner

This thesis was submitted to the Department of Mechatronic Engineering and is accepted as a fulfilment of the requirement for the degree of Master of Science (Mechatronic Engineering).

.....  
Ali Sophian  
Head, Department of Mechatronics  
Engineering

This dissertation was submitted to the Kulliyyah of Engineering and is accepted as a fulfilment of the requirement for the degree of Master of Science (Mechatronic Engineering).

.....  
Sany Izan Ihsan  
Dean, Kulliyyah of Engineering

## DECLARATION

I hereby declare that this thesis is the result of my investigations, except where otherwise stated. I also declare that it has not been previously or concurrently submitted as a whole for any other degrees at IIUM or other institutions.

Muhammad Mukhlis bin Suhaimi

Signature:.....

Date:.....1/3/2023.....

**INTERNATIONAL ISLAMIC UNIVERSITY MALAYSIA**

**DECLARATION OF COPYRIGHT AND AFFIRMATION OF  
FAIR USE OF UNPUBLISHED RESEARCH**

**STUDY OF HIGH-DENSITY EMG SIGNAL-BASED THUMB  
ATTITUDE RELATIONSHIP TO EXTRINSIC MUSCLES  
CHARACTERIZATION**

I declare that the copyright holder of this thesis are jointly owned by the student and IIUM.

Copyright © 2023 Muhammad Mukhlis bin Suhaimi and International Islamic University Malaysia. All rights reserved.

No part of this unpublished research may be reproduced, stored in a retrieval system, or transmitted, in any form or by any means, electronic, mechanical, photocopying, recording or otherwise without prior written permission of the copyright holder except as provided below

1. Any material contained in or derived from this unpublished research may only be used by others in their writing with due acknowledgement.
2. IIUM or its library will have the right to make and transmit copies (print or electronic) for institutional and academic purpose.
3. The IIUM library will have the right to make, store in a retrieval system and supply copies of this unpublished research if requested by other universities and research libraries.

By signing this form, I acknowledged that I have read and understand the IIUM Intellectual Property Right and Commercialization policy.

Affirmed by Muhammad Mukhlis bin Suhaimi



1/3/2023

## ACKNOWLEDGEMENTS

To Allah, the Almighty, whose Grace and Mercies have sustained me during my study, be all the honour. The process of finishing this thesis has been challenging, but His Mercies and Blessings on me have made it easier.

I would like to thank my supervisor, Aimi Shazwani binti Ghazali who gave many opinions that helped towards the success of this study. With patience, thoroughness, friendship, her detailed comments, and helpful suggestions have launched and facilitated the study so that I can complete this thesis and also successfully publish journals and conference papers. I am also grateful to my co-supervisor, Ahmad Jazlan bin Haja Mohideen and Prof. Shahrul Na'im bin Sidek whose support and cooperation contributed to the outcome of this work. The moral support they gave me was certainly a motivation that helped the construction and writing of this research work draft. Thank you also to all of the laboratory members who shared their knowledge and helped with data collection for this study.

Lastly, my gratitude goes to my beloved parents; for their prayers, understanding, encouragement and moral support throughout my studies.

We praise Allah once more for His unending kindness toward us, one of which is allowing us to successfully complete the writing of this thesis. Alhamdulillah.



# TABLE OF CONTENTS

Abstract .....	ii
Abstract in Arabic .....	iii
Approval Page.....	iv
Declaration.....	vi
Acknowledgements.....	viii
Table of Contents .....	ix
List of Tables .....	xi
List of Figures .....	xii
List of Symbols.....	xiv
<b>CHAPTER ONE: INTRODUCTION .....</b>	<b>1</b>
1.1 Background of Study .....	1
1.2 Problem Statements .....	5
1.3 Research Objective .....	6
1.4 Research Methodology .....	7
1.5 Scope of Research.....	10
1.6 Thesis Organization.....	10
1.7 Thesis Contribution .....	11
<b>CHAPTER TWO: LITERATURE REVIEW.....</b>	<b>12</b>
2.1 Introduction.....	12
2.2 Anatomy of Muscles.....	12
2.2.1 Intrinsic Muscles.....	13
2.2.2 Extrinsic Muscles.....	14
2.3 Electromyography (EMG).....	16
2.3.1 High-Density Surface EMG (HD-sEMG) .....	17
2.3.2 Electrode Placement.....	19
2.4 Feature Extraction.....	21
2.5 Classifier.....	22
2.6 Summary.....	25
<b>CHAPTER THREE: RESEARCH METHODOLOGY .....</b>	<b>26</b>
3.1 Introduction.....	26
3.2 System Design .....	26
3.3 Trajectory.....	29
3.4 Data Collection Procedure.....	33
3.5 HD-sEMG Recording Setup.....	36
3.6 Feature Extraction.....	39
3.7 Software Interface and Data Extraction.....	41
3.8 Normalization Data.....	46
3.9 Classifier .....	47

3.10	Summary.....	50
<b>CHAPTER FOUR: RESULT AND DISCUSSION .....</b>		<b>51</b>
4.1	Introduction.....	51
4.2	Participant.....	51
4.3	Statistical Analysis.....	53
4.3.1	Correlation Analysis.....	54
4.3.2	Interaction Effect.....	54
4.4	HD-sEMG Map .....	54
4.5	The Best Features and Classifiers.....	56
4.6	Details of the Best Classification Result .....	61
4.7	Confusion Matrix and Average Each Condition .....	63
4.8	Validation Result .....	67
4.9	Summary.....	70
<b>CHAPTER FIVE: CONCLUSION AND RECOMMENDATIONS .....</b>		<b>71</b>
5.1	Conclusion.....	71
5.1.1	To Upgrade an Existing Portable Thumb Muscles Platform and Establish a Standard sEMG Recording Setup for the HD-sEMG Patch for Consistent Measurement of Signals From the Forearm Musculature .....	71
5.1.2	To Investigate the Signal For the Optimized Extraction Method and the Best Selection of Features. ....	72
5.1.3	To Determine the Best Classifier and Validate the Performance of the Developed System by Classifying HD-sEMG Data Collected... ..	72
5.2	Limitations and Recommendations for Future Works.....	73
5.2.1	Thumb Attitude .....	74
5.2.2	Hand Position or Posture .....	74
5.2.3	Amputee Subjects.....	75
5.2.4	HD-sEMG Recording Device.....	75
5.2.5	Dynamic Grip Transition.....	76
5.3	Publication.....	77
<b>REFERENCES.....</b>		<b>78</b>
<b>APPENDIX I: IREC APPROVAL.....</b>		<b>87</b>
<b>APPENDIX II: CONSENT FORM.....</b>		<b>89</b>

## LIST OF TABLES

Table 2.1	Intrinsic muscles description	13
Table 2.2	Extrinsic muscles description	15
Table 2.3	Classifier and result used in earlier researchers. Linear discriminant analysis (LDA), Structural Similarity Index (SSIM), support vector machines (SVM), k-Nearest Neighbours (KNN), Gaussian mixture mode (GMM).	24
Table 3.1	Denotation of Thumb Posture Classes	48
Table 4.1	Result of 30% MVC each attitude for each subject	52
Table 4.2	Classification result for RAW and normalized data for each classifier	57
Table 4.3	Average of the normalized result	58
Table 4.4	Both hand sides result for classifier LDA and KNN	60
Table 4.5	Confusion matrix for RMS data from the anterior and posterior hand sides	63
Table 4.6	Confusion matrix for ARV-RMS data from the anterior and posterior hand sides	64
Table 4.7	Classification results for anterior-posterior hand sides	65
Table 4.8	Summary of correctly classified instances based on conditions and attitudes	67
Table 4.9	Confusion matrix for training data set	68
Table 4.10	Confusion matrix for testing data set	69
Table 4.11	Confusion matrix for validation data set	69
Table 4.12	Confusion matrix for all data set	70

## LIST OF FIGURES

Figure 1.1	Transradial and Transcarpal	2
Figure 1.2	Positions of the electrodes; (1) AP, (2) FPB, (3) APB, (4) FDI	3
Figure 1.3	(Left) Muscles in the <b>anterior</b> compartment of extrinsic muscles (flexor muscles of the forearm). The muscles of the anterior compartment of the forearm are depicted in this image from the deepest layer (left) to the most superficial one (right) (Right) Muscles in the <b>posterior</b> compartment of extrinsic muscles (extensor muscles of the forearm). The muscles of the posterior compartment of the forearm are depicted in this image moving from the deepest to the most superficial layer	4
Figure 1.4	Flow chart of the methodology	9
Figure 2.1	Intrinsic Muscles	14
Figure 2.2	Extrinsic muscles	16
Figure 2.3	RGB color replicated different amplitude EMG signal captured by HD-sEMG electrode in the form of bi-demension picture	19
Figure 2.4	Placement electrode used by Aranceta-Garza and Conway (2019)	20
Figure 2.5	(Top) Active points in the anterior compartment (Bottom) Active points in the posterior compartment. The active points also slightly change when the position of the hand changes from supination to neutral on the anterior compartment and pronation	21
Figure 3.1	Portable Thumb Training System	27
Figure 3.2	Angle block diagram	28
Figure 3.3	Thumb attitudes	28

Figure 3.4	Trajectory interface	30
Figure 3.5	Force block diagram	31
Figure 3.6	Desired graph parameter	33
Figure 3.7	Procedures for data collection	34
Figure 3.8	Electrode placement standard	35
Figure 3.9	Experiment setup to collect the HD-sEMG signals recording	35
Figure 3.10	Sessantaquattro by OT-Bioelettronica	37
Figure 3.11	HD-sEMG electrode	38
Figure 3.12	HD-sEMG electrode foam	38
Figure 3.13	HD-sEMG software setting	39
Figure 3.14	OTBioLab data interface	42
Figure 3.15	Signal interface details	43
Figure 3.16	Offline processing direction (feature extraction)	44
Figure 3.17	Feature extracted interface	45
Figure 3.18	Feature extracted interface details and export direction	46
Figure 3.19	Classifier setting	49
Figure 4.1	Average force applied at 30% MVC in each posture	53
Figure 4.2	HD-sEMG activation maps at each thumb posture for Subject 6 using ARV and RMS features	55
Figure 4.3	Summary of correctly classified instances for ARV, RMS and their combinations based on hand sides	61

## LIST OF SYMBOLS

EMG	Electromyogram
sEMG	Surface Electromyography
HD-sEMG	High-Density Surface Electromyogram
AP	Abductor Pollicis
FPB	Flexor Pollicis Brevis
OP	Opponens Pollicis
FDI	First Dorsal Interosseous
MVC	Maximum Voluntary Contraction
GUI	Graphical User Interface
TD	Time Domain
FD	Frequency Domain
ARV	Absolute Rectified Value
MAV	Mean Absolute Value
RMS	Root Mean Square
KNN	K-Nearest Neighbour
TPR	True Positive Rate
FN	False Negative

# CHAPTER ONE

## INTRODUCTION

### 1.1 BACKGROUND OF THE STUDY

The human hand is an important body part that is used to control and handle daily activities such as grasping, pinching, and gripping (Yan Li, 2019). For normal people, the hand has five digits which consist of four fingers and a thumb. According to WHO (World Health Organization, 2004), 0.5% of the population in a developing country has a disability that necessitates the use of a prosthesis or orthosis. This prediction suggests that approximately 160,000 of Malaysia's current population of 32 million require prosthetic or orthotic devices. In addition, based on a record, there are approximately 1.6 million individuals living with limb loss in the United States, and it is estimated that the number will double by 2050 (Ziegler-graham et al., 2008). The common loss of limbs is due to accidents, wars, and diseases. There are also congenital cases where a person is born without a fully functional hand. These groups of people are known as amputees.

There are two categories of amputees, namely transradial and transcarpal. As demonstrated in Figure 1.1, transradial amputation occurs in the forearm area, in which the incisions are typically made on a ratio of 1 to 1 of the forearm length. It may cause the loss of interconnection between two main types of muscles, namely the intrinsic and extrinsic muscles. Meanwhile, transcarpal amputation is a common type of amputation that occurs for a variety of reasons such as diabetes and accidents, which in some cases will eventually result in amputation (removal through surgery). In general, more hand muscle activity data can be extracted from transcarpal amputees than transradial amputees since the flexion and extension of the wrist are still preserved. As such, transcarpal amputees can achieve higher

recovery of overall hand function compared to transradial amputees (Maduri & Akhondi, 2020).

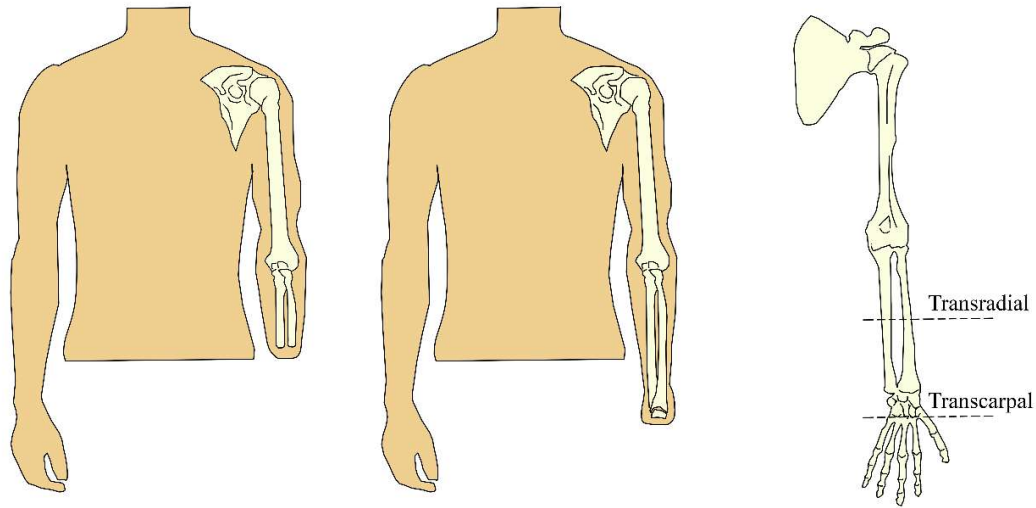


Figure 1.1: Transradial and Transcarpal

Research findings in neurophysiology and neuroscience have been utilised in the latest surgical procedures to incorporate prosthetic elements such as hand prostheses, osseointegration and myo-controllers (Kanitz et al., 2018). Over the last decade, earlier researches have achieved significant progress in the field of prosthetic hand development that utilises Electromyogram (EMG) measurements (Sánchez-velasco et al., 2019), which have given huge benefits to amputees in assisting in their daily activities to resemble normal limb functions. Based on one study (Cordella et al., 2016), hand prostheses are typically controlled by the sampling features taken from surface Electromyography (sEMG) signals obtained from the amputee's limb residual muscles. There are two types of EMG, namely invasive and non-invasive. Non-invasive sEMG is more common in prosthesis development (Chowdhury et al., 2013) and clinical usage, such as in physiology (Enoka, 2019), as this technique is painless and easily reproducible.



The thumb is the first digit of the human hand which is also known as *pollex* in its scientific term. Since the thumb is the only opposable digit to the other four fingers, it plays a critical role in hand function. Controlling this finger is vital for the realisation of different hand grip attitudes. Also, the contribution of the thumb towards hand functions and movements is inherently indispensable since the thumb is the only opposable digit that controls grip formation. Injury or loss of function of the thumb can severely limit overall hand function and movement (Xu et al., 2018).

To control and maximise the attitude and force of this digit, the thumb demands a combination activation of all the connected muscles (Drake et al, 2015; Wohlman & Murray, 2013). Critically, the thumb cannot be simulated accurately via individual intrinsic muscle contribution (Wohlman & Murray, 2013). The technique to record the sEMG signal to replicate thumb gestures is centred on the thumb musculature by measuring the activities of the intrinsic muscle in the palm area as demonstrated in Figure 1.2. The other extrinsic muscles governing the thumb lie on the forearm as shown in Figure 1.3. This interplay between extrinsic and intrinsic muscles is mostly reduced or lost for transcarpal and transradial amputees. Yet, the remaining residual forearm muscles (the extrinsic muscles) are still accessible for both types of amputees and could be useful to control a myoelectric-based prosthetic hand.

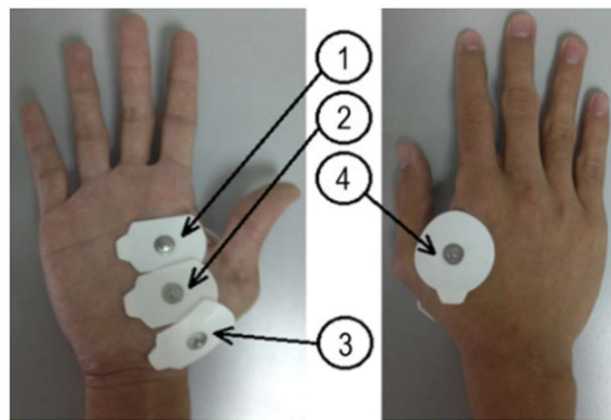


Figure 1.2: Positions of the electrodes; (1) AP, (2) FPB, (3) APB, (4) FDI (Sidek et al., 2018)

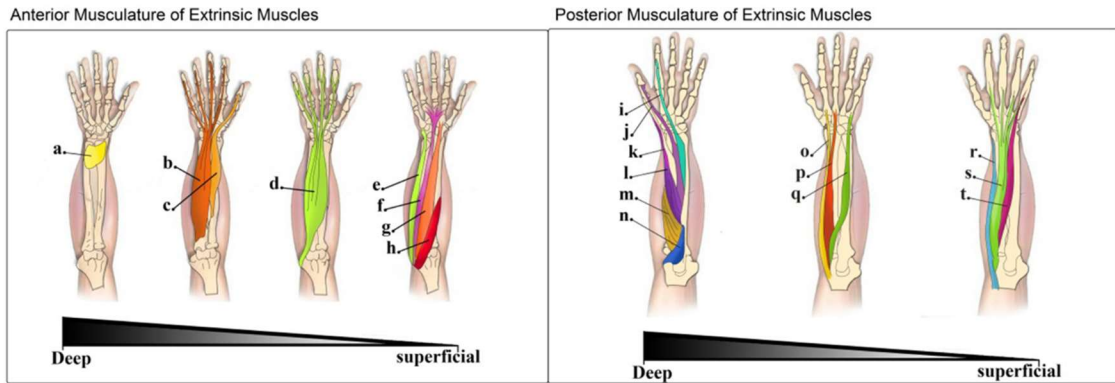


Figure 1.3: (Left) Muscles in the **anterior** compartment of extrinsic muscles (flexor muscles of the forearm). The muscles of the anterior compartment of the forearm are depicted in this image from the deepest layer (left) to the most superficial one (right)

(Right) Muscles in the **posterior** compartment of extrinsic muscles (extensor muscles of the forearm). The muscles of the posterior compartment of the forearm are depicted in this image moving from the deepest to the most superficial layer (Aranceta-Garza and Conway, 2019)

The biomechanics of the skeleton, thumb joint, and muscle-tendon action of the extrinsic muscle are the factors that influence thumb activities. Due to the lack of detailed studies on other factors influencing thumb characteristics, biomechanical prosthetics have limitations in function and performance (Wohlman & Murray, 2013; Xu et al., 2018). These limitations of prosthetics can cause phantom or telescoped sensations on the amputees' remaining hand limb. Phantom is a situation in which the proximal limb has shrunk, where in some cases, the amputees feel as if the limb is still present (Wijk & Carlsson, 2015).

There are continuous developments in cybernetic hands that can help create improved hand prostheses for transradial and transcarpal amputees (Wijk & Carlsson, 2015). As it is a crucial need for disabled individuals, opportunities for research and

development on these cybernetic hands are still open for further improvements. With a newer EMG technology called the High-Density surface Electromyogram (HD-sEMG), existing technologies can be further improved. The HD-sEMG uses multiple electrodes that are arranged in a specific array. Previous studies (Ammal et al., 2015; Stegeman et al., 2012) have shown that the effect of electrode numbers on recognition performance improves recognition accuracy.

## **1.2 PROBLEM STATEMENT**

There are millions of hand amputees around the world, and unfortunately, these numbers increase each year. Hand prosthetics provide some functionalities of the human hand for amputees. However, current prosthetic hands lack accuracy in replicating hand gestures due to the lack of information that can be extracted from the muscles. Centring on the thumb, there are still gaps in research that focus on the synergy of targeted muscles on thumb movements.

Additionally, the limited information obtained from the placement of conventional sEMG electrode results in insufficient representations of overall muscle activity (Garcia and Vieira, 2011). As a result, smooth movements especially for prosthetic hand applications are hard to achieve due to the missing data from the targeted muscles.

Importantly, the main muscles that control the thumb attitude are the five intrinsic muscles that have easy access to the thumb. The other four extrinsic muscles that govern the thumb are located in the deep compartment of the forearm and contribute indirectly to thumb attitude. Despite the loss of access to the intrinsic muscles, any information from the extrinsic muscles is non-negotiable for transradial amputees.

Previous studies have focused on specific thumb attitudes, especially on abduction (Aranceta-Garza and Conway, 2019). However, different attitudes such as flexion and extension as presented in this work have not yet been covered.

### **1.3 RESEARCH OBJECTIVE**

The main objective of this research, therefore, is to investigate (and establish) the relationship between the synergy of the HD-sEMG signal from extrinsic musculature and the thumb postures to be replicated on prosthetic hands for transradial amputees.

The main objective can be divided into four sub-objectives as follows:

- 1) To upgrade an existing portable thumb muscles platform and establish a standard sEMG recording setup for the HD-sEMG patch for consistent measurement of signals from the forearm musculature.
- 2) To determine the optimised feature extraction method and the best selection of features for the HD-sEMG data collected.
- 3) To determine the best classifier and validate the performance of the developed system by classifying HD-sEMG data collected.

## **1.4 RESEARCH METHODOLOGY**

The execution plan for the research has been divided into five phases. An overview of the methodology, including the methods and materials of the experimental design, is described as follows and is summarised in Figure 1.4;

### **1.4.1 Phase-I**

1. Conduct a comprehensive review of the existing literature on the development, design, control, implementation, and application of prosthetic limbs (particularly hand and thumb prostheses).
2. Study the related thumb muscles and finalise the targeted muscles.
3. Request for ethical clearance from the IIUM Research Ethics Committee (ID no: IREC 2020-080).

### **1.4.2 Phase-II**

1. Upgrade the existing thumb measurement system to accommodate different thumb postures, specifically for flexion activities. Set four different postures for the study: zero-degree, thirty-degree, sixty-degree, and ninety-degree angles.
2. Finalise the experimental protocol needed for the collection of raw data sets of HD-sEMG signals. The protocol includes data collection procedures, electrode placement, and the number of records for each subject.

3. Test the system on pilot subjects (members of BioMechatronics Lab). Improve the necessary study protocol besides analysing and evaluating the results.
4. Purposively sample and select 17 subjects among IIUM students with no huge accident history and disease on the targeted hand that may affect the result.

### **1.4.3 Phase-III**

1. Finalise the set up for the thumb measurement system and the experimental procedure to collect HD-sEMG data from the subjects' forearm musculature at different thumb postures.
2. Perform feature extraction in terms of time domain and frequency domain analysis, followed by selecting the features that yield the highest correctly classified instances using several classifiers.
3. Apply classification techniques to establish the relationship between HD-sEMG signal features and various thumb angles (flexion activities). Finalise an appropriate classifier based on the highest percentage of correctly classified data to classify the collected data.

### **1.4.4 Phase-IV**

1. Formulate the conclusions of the study and recommendations for future works.
2. Write a final thesis and publish several journal and conference papers.

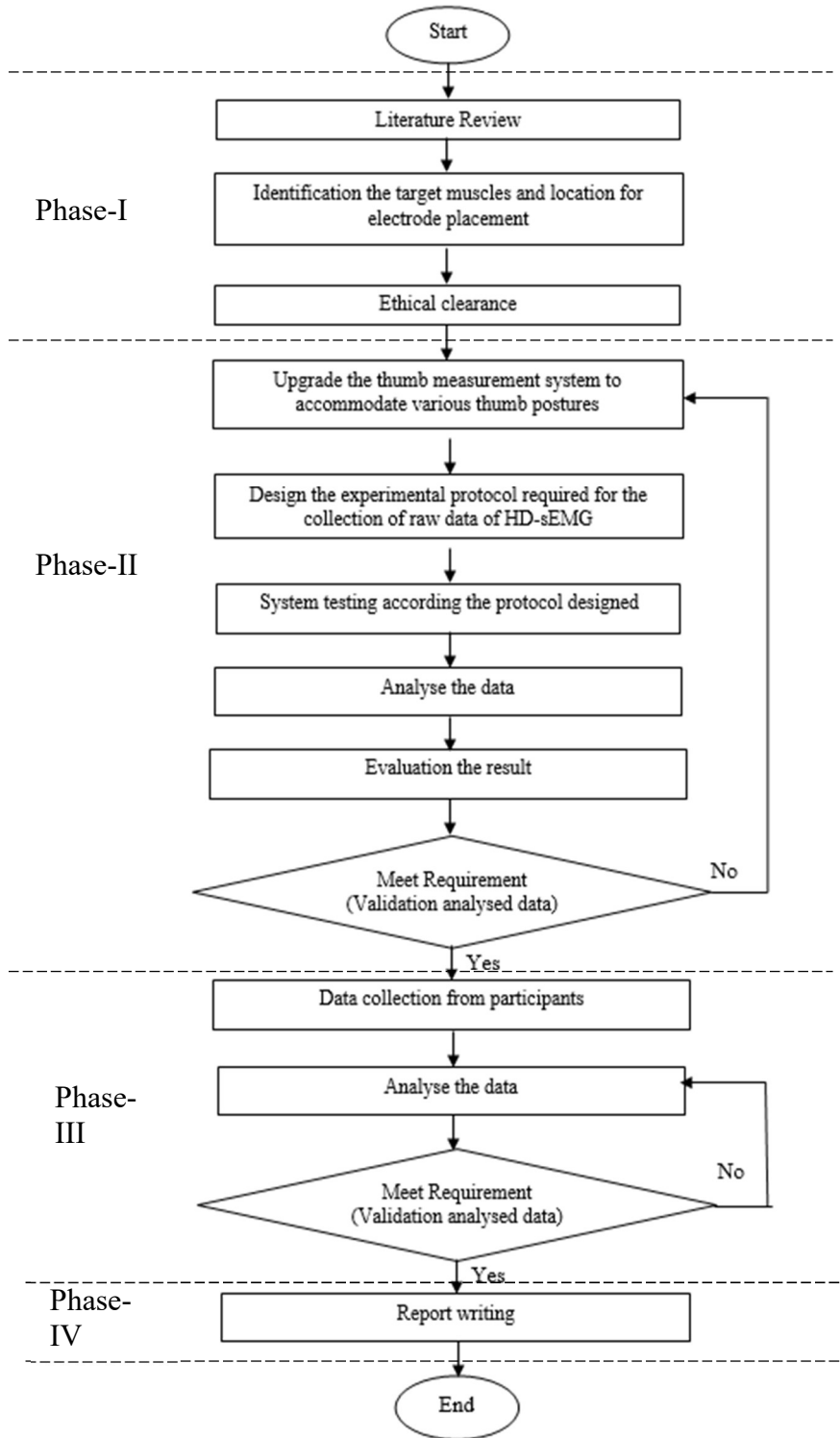


Figure 1.4: Flowchart of the methodology

## **1.5 SCOPE OF RESEARCH**

The scope of the study is as follows:

1. This study to investigate the synergy of EMG signal from forearm with thumb attitude begins with upgrading the portable thumb training system platform to replicate four different thumb attitudes for flexion activities and the methods finalised for HD-sEMG data collection procedures by the forearm of the healthy subject targeting on the right hand.
2. Recruiting 17 subjects from the IIUM students with good health and no accident history and/or diseases on the targeted hand and each participant will be completed the collecting data procedure
3. Examining the features for time domain (TD) and frequency domain (FD) analyses (root mean square (RMS), mean absolute value (MAV), mean frequency (MNF) and median frequency (MDF)) and evaluating the results based on selected classifiers only (linear discriminant analysis (LDA), support vector machine (SVM), k-Nearest Neighbour (KNN), and TREE-based classifier). Then the collected data are analysed with classifying different thumb attitudes using machine and deep learning, and classification learner app in Matlab R2020.

## **1.6 THESIS ORGANISATION**

The thesis is divided into five chapters:

Chapter 1: Describes the overview of the research by discussing the problem statements, research objective, methodology, and scope of the research.



Chapter 2: Presents a literature review related to several studies on the muscles (intrinsic and extrinsic) that contribute to controlling the thumb and steps for data analyses including feature extraction and selection of classifiers.

Chapter 3: Elaborates on the research methodology used in the study.

Chapter 4: Discusses the outcomes from the analyses of HD-sEMG signals for several selected features and classifiers.

Chapter 5: Details the achievement of the objectives, limitations of the study, and recommendations for future works.

## **1.7 THESIS CONTRIBUTION**

The current thesis contributes to the knowledge of HD-sEMG signals' patterns in replicating thumb attitude specifically for flexion activity in designing advanced hand prostheses. The previous study show limitation on the selected methods and effected on the accuracy of the classifier result and gap on the attitude of the thumb study. In this thesis, we provide an elaborate account of how the procedure was conducted. The work includes electrode placement and data collection procedures for flexion activity, feature extraction and classification. This thesis discussed with details on the result leads to the best selection features and classifier for the collected data. In short, the research contributes to the study of HD-sEMG signals in classifying different thumb attitudes, specifically on flexion activity for contract and relax activities.

## **CHAPTER TWO**

### **LITERATURE REVIEW**

#### **2.1 INTRODUCTION**

The thumb is the only opposable digit of the human hand and it is primarily important to perform any hand gestures. The digits are controlled by a combination of different muscles located within the forearm and hands. sEMG-related technology has been previously used to analyse both the thumb and other digit muscle activities. In this chapter, earlier works on prosthetic technology, gesture control by EMG, and further details of EMG technology, are discussed. Signal processing steps including feature extraction from the captured HD-sEMG electrodes (the raw data) and the classification process is also elaborated accordingly. At the end of the chapter, a summary of the key highlights to be used throughout the research is provided.

#### **2.2 ANATOMY OF MUSCLES**

Individual fingers move biomechanically using muscles that have different anatomical compartments and separate tendons. When combined with other digits, standard handgrip activities are achieved. The thumb is the only opposable digit responsible for the majority of hand functions (Xu et al., 2018). The thumb muscles can be divided into two parts, namely intrinsic (hand) and extrinsic (forearm) muscles.

### 2.2.1 Intrinsic Muscles

The thumb has a distinct feature from other digits, where for the four other digits, the main movements are bidirectional, namely flexion and extension. Meanwhile, the thumb has at least four movements, namely adduction, abduction, flexion, and extension (Adewuyi et al., 2016). The majority of the main muscles of the thumb are located in the hand (palm) and are also known as intrinsic muscles. The activation of the intrinsic thumb muscles located close to the skin's surface of the hand determines both the grip strength and thumb attitude (Xu et al., 2018). Each of these intrinsic muscles serves an individual purpose as presented in Table 2.1, while the combination of these intrinsic muscles play a major role in carrying out daily activities. Figure 2.1 depicts a diagram of hand anatomy which consists of five intrinsic muscles, namely *Abductor Pollicis*, *Flexor Pollicis Brevis*, *Abductor Pollicis Brevis*, *Opponens Pollicis* and *First Dorsal Interosseous* (Aranceta-Garza and Conway, 2019; Drake et al, 2015). Since these muscles are the main muscles used in controlling thumb attitude, classification of muscle activations, thumb attitude, and strength is required from these muscles.

Table 2.1: Intrinsic muscles description

<b>Muscles name</b>	<b>Contribution</b>
<i>Abductor Pollicis</i>	Thumb adduction
<i>Flexor Pollicis Brevis</i>	Thumb flexion
<i>Abductor Pollicis Brevis</i>	Thumb adduction
<i>Opponens Pollicis</i>	Thumb opposition
<i>First Dorsal Interosseous</i>	Thumb flexion and extension

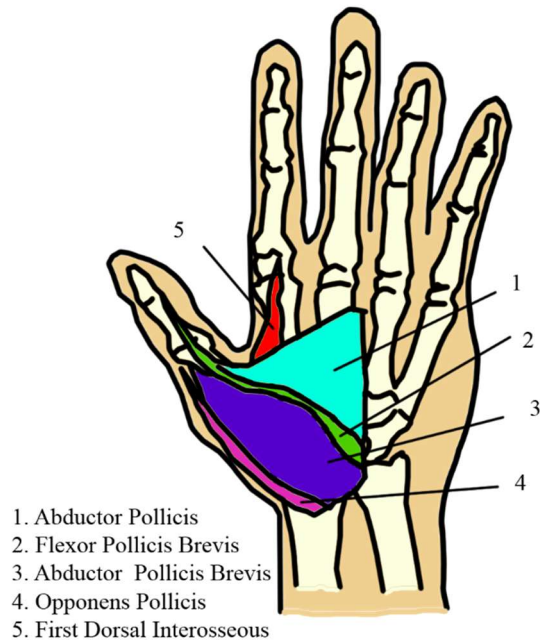


Figure 2.1: Intrinsic Muscles

### 2.2.2 Extrinsic Muscles

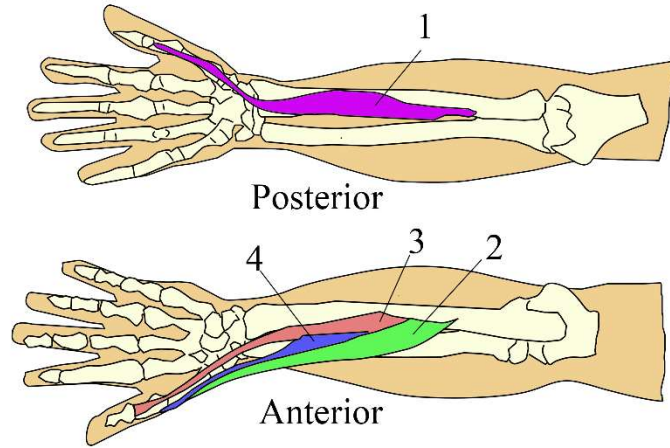
Hand functions and finger movements are predominantly controlled by the extrinsic muscles located in the forearm. Extrinsic muscles consist of several muscles that perform various functions as summarised in Table 2.2. For amputees, information from extrinsic muscles can be used to replicate the thumb attitude and potentially be used for conventional myoelectric prosthesis control (Adewuyi et al., 2016). The extrinsic muscles which directly contribute to thumb attitude are illustrated in Figure 2.2.

The *Flexor Pollicis Longus*, which is located in the deepest layer of the muscles, is the target muscle that controls the thumb digit on the anterior side. On top of this muscle, there are two layers of muscles which consist of five other muscles (*Flexor Carpi Ulnaris*,

*Palmaris Longus; Flexor Carpi Radialis, Pronator Teres*) (Aranceta-Garza and Conway, 2019; Xu et al., 2018). These muscles contribute to the activity of thumb flexion. Notably, there is only one muscle that contributes to the different thumb attitudes on the anterior side. Meanwhile, there are three muscles that are connected to the thumb on the posterior side, namely the *Abductor Pollicis Longus*, *Extensor Pollicis Brevis*, and *Extensor Pollicis Longus*. All of these muscles are located next to the other three muscles in the deepest layer of the posterior forearm. The *Abductor Pollicis Longus* contributes to the abduction and extension of the thumb (*Abductor Pollicis Longus - Physiopedia*, n.d.), the *Extensor Pollicis Brevis* controls thumb abduction (Jabir et al., 2013), and the *Extensor Pollicis Longus* contributes to the extension of the interphalangeal joint of the thumb (*Extensor Pollicis Longus - Physiopedia*, n.d.). Above these muscles, two more layers of muscles contribute to different finger functions and this creates challenges in capturing the targeted muscle signal for both sides of the hand (anterior and posterior sides).

Table 2.2: Extrinsic muscles description

<b>Muscles name</b>	<b>Contribution</b>
<b>Flexor Pollicis Longus</b>	Thumb flexion
<b>Abductor Pollicis Longus</b>	Thumb abduction and extension
<b>Extensor Pollicis Longus</b>	Thumb extension
<b>Extensor Pollicis Brevis</b>	Thumb extension



- |                             |                             |
|-----------------------------|-----------------------------|
| 1. Flexor Pollicis Longus   | 3. Extensor Pollicis Longus |
| 2. Abductor Pollicis Longus | 4. Extensor Pollicis Brevis |

Figure 2.2: Extrinsic muscles

### 2.3 ELECTROMYOGRAPHY (EMG)

EMG is a type of bio-signal that represents neuromuscular activities by measuring the electrical current generated in the muscles (Li et al., 2015) during muscle activity. When the thumb exerts a certain amount of force, the EMG signals from related muscles can be captured. Before amplification, the amplitude range of the raw EMG signal varies between 0 to 10mV ( $\pm 5$ mV) and these voltage values are directly proportional to the force applied (Mohideen & Sidek, 2011); (Arnold et al., 2013). Studies have shown that ion flow through muscle fibres has a significant influence on the force exerted and is directly reflected in the EMG data collected (Arnold et al., 2013; Dai & Hu, 2019; Ghaderi & Marateb, 2017). Even though myoelectric prosthetics have increased flexibility and anthropomorphism of the thumb, the control mechanism for this digit through sEMG has remained unchanged over the last four decades (Mastinu et al., 2019).

### **2.3.1 High-Density Surface EMG (HD-SEMG)**

One of the highlighted advantages of sEMG over intramuscular EMG (or known as needle EMG) is that it is widely reproducible in follow-up studies due to its non-invasiveness and relative ease in collecting spatial distributions of data. Continuous research and development have revealed limitations in the analysis of sEMG, such as limited information from the placement of the electrodes, which results in insufficient representations of the overall activity of the muscles (Garcia and Vieira, 2011). These limitations have led to an improved technology known as the HD-sEMG (Stegeman et al., 2012). HD-sEMG has many similarities to ordinary sEMG measurements, the main difference being that smaller electrodes are densely arranged in a grid position along the region of interest, which enables more information to be obtained from the region of muscles under investigation. Multiple electrodes used to sample EMG activity from a single muscle are expected to provide valuable insights into muscle physiology and anatomy (Vieira & Botter, 2021). Thus, HD-sEMG does not limit access in case more data are required to be captured from multiple targeted muscles (Garcia and Vieira, 2011) at one time.

A study conducted by Garcia and Vieira (2011) highlighted some advantages of using HD-sEMG compared to normal surface EMG. The first advantage is based on the myoelectric activity detected and further physiological indications that can be obtained when multiple electrodes are used at the location of tendons and end-plates, as well as the length of muscle fibres. Also, by using HD-sEMG, the actual position of the muscles can be detected more accurately than sEMG. Thus, the problem of placement mismatch for a single sEMG can be overcome. In addition, when an array of surface electrodes is placed on the skin parallel to the path of the muscle fibres, each electrode will report a delayed representation of the Motor Unit Action Potentials. Therefore, the conduction velocity of action potentials propagated along the muscle fibres can only be measured afterwards. Interestingly, this delay can be minimised or omitted using HD-sEMG technology (Ghaderi & Marateb, 2017).

The HD-sEMG uses multiple electrodes arranged in a specific array. Previous studies (Amma et al., 2015; Stegeman et al., 2012) have shown the effect of electrode numbers on recognition accuracy. The array is used to measure the propagating potential at various spatial positions along the course of the muscle fibres. As a result, more comprehensive muscular activity data can be obtained using HD-sEMG as compared to conventional sEMG. Furthermore, the usage of HD-sEMG can address the placement mismatch of electrodes that occurs in conventional sEMG (Garcia and Vieira, 2011). HD-sEMG also enables high-accuracy estimation of the innervation zone location, as well as an estimation of muscle fibres conduction velocity, length, and orientation (Ghaderi & Marateb, 2017).

Using HD-sEMG, electrical activities present on the skin's surface can be recorded using the bi-dimension technique in developing a map (Nait-ali et al., 2019) as illustrated in Figure 2.3. The map is an image in which each pixel represents each electrode for HD-sEMG. The data or signal extracted from these muscle activity maps is required to identify active areas during the movements of targeted muscles. The segmentation is beneficial for clinical neurophysiology in monitoring muscle activities. Also, it is instrumental in the usage of robotic-assisted therapies and prosthetic hands (Amma et al., 2015; Nait-ali et al., 2019). As shown in Figure 2.3, interpolation maps are commonly used when displaying muscle activation as spatial resolution increases.



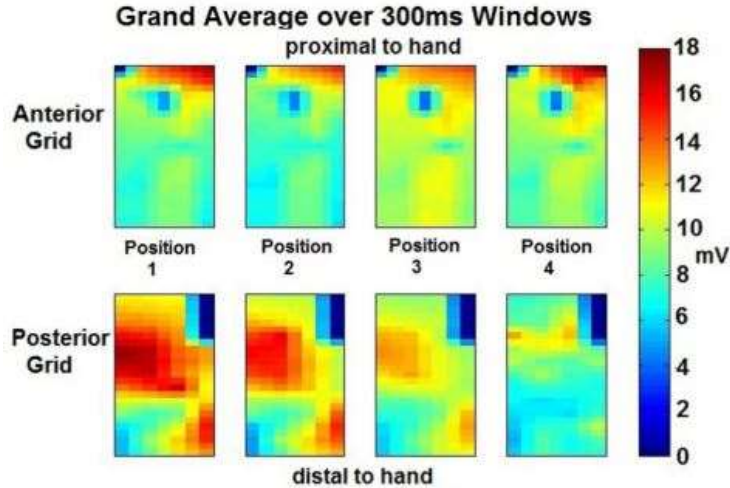


Figure 2.3: RGB colour replicated different amplitude EMG signals captured by HD-sEMG electrode in the form of a bi-dimension picture representing four different positions corresponding to 4 digits: secundus digitus manus, digitus medius, digitus annularis, and digitus minimus manus, respectively (Aranceta-Garza and Conway, 2019).

### 2.3.2 Electrode Placement

EMG signals are subjected to noise from various sources. Cables connected to the electrodes may pick up noise from the main electricity supply. Motion artefacts may also contaminate the EMG signals. Careful electrode placement can mitigate the effects of noise. The EMG amplitude signal depends highly on the location of the electrode placement (Bao et al., 2018; Xu et al., 2018). The standard placement of the electrode used by (Aranceta-Garza and Conway, 2019) is proximally 25% from the ulnar head and the olecranon for the posterior view and the ulnar head to the elbow crease for the anterior view as shown in Figure 2.4. The electrode used is a 13-by-5 electrode grid (with an approximately 13cm-by-5cm coverage area of the signal reception).

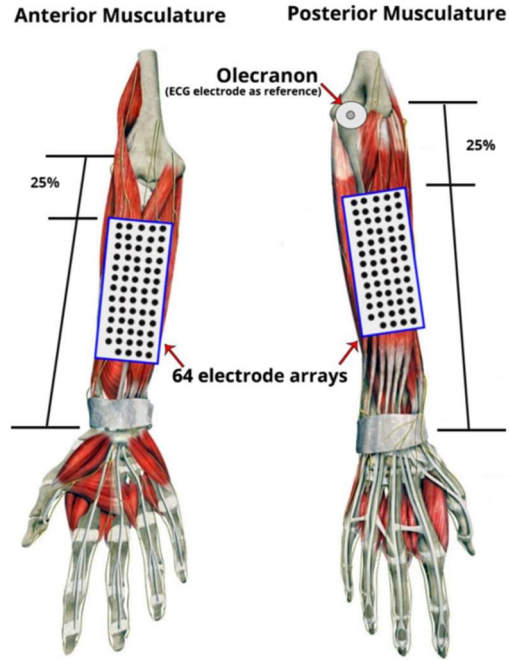


Figure 2.4: Placement electrode used by Aranceta-Garza and Conway, (2019)

Bao et al., (2018) focused on the placement of an electrode on the forearm to stimulate finger extension or flexion. The focus of the research was to compare electrode positions and forearm rotation which affect the activation threshold. The study also developed a theoretical model of electrode placement for the selective activation (extension or flexion) of individual fingers. As a result, the activation of the thumb during the extension or flexion is accumulated at the middle of the forearm to the side of the radius bone approximately 4cm from the wrist as shown in Figure 2.5. In conclusion, the electrode placement used by Aranceta-Garza and Conway, (2019) agrees with the outcomes by Bao et al., (2018).

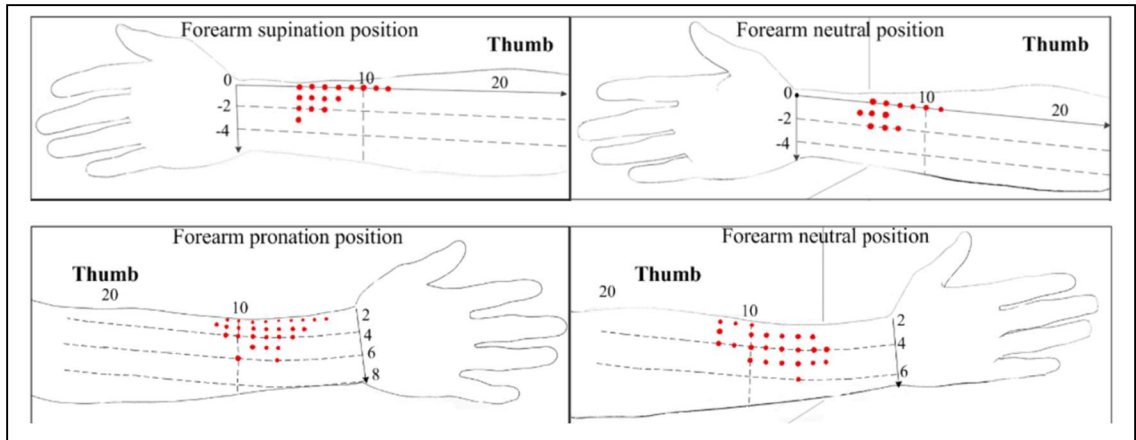


Figure 2.5: (Top) Active points in the anterior compartment. (Bottom) Active points in the posterior compartment. The active points vary when the position of the hand changes from supination to neutral on the anterior compartment and pronation.

## 2.4 FEATURE EXTRACTION

The collected signal from the targeted area is in the raw data. To extract valuable information from raw data, there is a step called feature extraction, where the most significant features are fed to a classifier to form classes for the dataset (Inam et al., 2021; Toledo-Pérez et al., 2019). Features can be extracted using TD, FD, and combined time-frequency domains. Due to its mathematical simplicity and good performance, TD features are commonly used (Hakonen et al., 2015; Inam et al., 2021). TD features are determined based on the amplitude of the signals and do not require any extensive computations. Commonly used TD features are RMS (Aranceta-Garza and Conway, 2019; Higashi et al., 2019) and MAV (Bi et al., 2020; Turgunov et al., 2020). FD characteristics are based on the frequency range and are calculated using Fourier transformations. Commonly used FD features are MNF (M. M. Alam et al., 2020; Dupan et al., 2018) and MDF (Alam et al., 2020; Goubault et al., 2021). The results of the study conducted by Siddiqi & Sidek, (2016) showed that TD analysis produces higher accuracy to differentiate different finger attitudes

than FD, which is better in classifying muscles' fatigue status. Also, TD is preferable to be used in the study of different hand attitudes' EMG-based signals.

## **2.5 CLASSIFIER**

Data classification is essential for developing a control algorithm for the cybernetic prosthesis. It is a useful technique to describe the behaviour of complex nonlinear processes in the presence of conventional mathematical models (Inam et al., 2021; Khan et al., 2020).

Classification algorithms are classified into three types: supervised learning, unsupervised learning, and reinforcement learning (Ghazali et al., 2015; Khan et al., 2020). In supervised learning, the algorithm has access to or is provided with the data it is attempting to predict. A classic example of supervised learning is the classification of animals, namely cats and fish. After collecting the features' information such as the presence of fur, scale, and ears on the animals' bodies, the data are fed into a classifier, for example, KNN, while labelling those data according to its classes (whether the specific data matches that of a cat or a fish). In contrast to supervised learning, there is no target value in an unsupervised learning task. For example, classification for customer segmentation. The process of understanding different customer groups to develop marketing or other business strategies based on customer demands. In contrast to reinforcement learning, this algorithm creates a system that can learn by interacting with the environment (Vieira et al., 2019) through reward and punishment concepts. For example, a rescue robot is designed to autonomously move in a building. As the time needed to escape the building is short, the robot will be rewarded every time it achieves a new record after trying several routes. In case the time recorded gets longer, the robot will be punished to show that the chosen route is wrong.

HD-sEMG has three specific methods of classification, namely the HD-EMG map intensity and centre of gravity classification, HD-EMG map intensity classification, and single differential channel intensity classification. All these techniques use supervised learning and classification based on the intensity of a single differential channel which is recommended as the best technique for classifying HD-sEMG data (Jordanic et al., 2016). Table 2.3 summarises the type of classifier and accuracy achieved in earlier studies in classifying HD-sEMG signals.

In the table below, various objectives from the previous study are listed. The selected papers have one thing in common, they all focus on data collected from the forearm area. The accuracy for the papers is greater than 90% except for the paper by Paul et al., (2017), which is a comparison of different classifiers.

Table 2.3: Classifier and result used in earlier researchers. LDA, Random Forest (RF), SVM, KNN

Author (year)	Title	Study's objective	Targeted area and dynamic factor	Classifier used	Results
(Yu et al., 2018)	Attenuating the Impact of Limb Position on Surface EMG Pattern Recognition Using a Mixed-LDA Classified	Investigated the effect of limb position variation on pattern recognition-based motion classification using a linear discrimination analysis (LDA) classifier	-Forearm area -Limb position	LDA	93.60%
(Celadon et al., 2016)	Proportional estimation of finger movements from high-density surface electromyography	Investigated finger force estimation using HD-sEMG to record the electrical activity of the extrinsic hand muscles during isometric finger flexion and extension	-Forearm area - Individual fingers (index, middle, ring and little)	LDA	91%
(Paul et al., 2017)	Comparative Analysis between SVM & KNN Classifier for EMG Signal Classification on Elementary Time Domain Features	Comparative analysis.	-Forearm -Six basic hand movement	kNN, SVM	SVM > kNN
(Islam et al., 2022)	Forearm Orientation and Muscle Force Invariant Feature Selection Method for Myoelectric Pattern Recognition	The proposed feature selection method would be very beneficial for identifying the least dimensional features and enhancing EMG-PR performance.	-Forearm area -Three orientation forearm	kNN, SVM, LDA	91.46% - 93.27%
(M. S. Alam & Arefin, 2018)	Real-Time Classification of Multi-Channel Forearm EMG to Recognize Hand Movements using Effective Feature Combination and LDA Classifier	The study's objective was to devise techniques for the quick and real-time classification of EMG signals obtained from hand movements.	-Forearm area -Different hand motion	LDA	96.5%
(Dai & Hu, 2019)	Extracting and Classifying Spatial Muscle Activation Patterns in Forearm Flexor Muscles Using High-Density Electromyogram Recordings	The objective of this study is to quantify the spatial patterns of forearm flexor muscle activation during individual finger flexions.	- Forearm area - Individual fingers (index, middle, ring and little)	LDA, SVM	96.76%

## 2.6 SUMMARY

This chapter introduced two types of muscles, namely intrinsic and extrinsic muscles, which contribute to thumb attitude and force exerted. Focusing on extrinsic muscles, this study aims to extract information from these muscles to replicate the thumb attitude for transradial amputees. Aside from that, the chapter discusses the features extracted from HD-sEMG used in previous studies, namely TD (RMS and ARV) and FD (MNF and MDF) features. The classifiers were used by previous researchers in the final focus of the literature review. It can be concluded that LDA, SVM and KNN are the three most used classifiers to analyse EMG signals in general.

## **CHAPTER THREE**

### **RESEARCH METHODOLOGY**

#### **3.1 INTRODUCTION**

To tackle the limitations of past studies as discussed in the earlier chapters, this study was designated to investigate the synergy between high-density EMG patterns at the forearm musculature based on four different thumb attitudes. The study's goals include forming standardised data collection procedures on the sEMG signals taken from the forearm for repeatable purposes and classifying those signals based on their thumb attitudes before implementing the thumb training system on transradial amputees (the real patients). As such, this chapter will discuss in detail the developed system, including the experiment setup, data collection procedure, feature extraction, normalisation, and classifier applied in categorising the collected sEMG signals.

#### **3.2 SYSTEM DESIGN**

As shown in Figure 3.1, the platform used to manipulate the thumb's angles in this was a portable thumb training system. The platform was made up of four major components which were a hand rest, an adjustable wrist position, a potentiometer, and a load cell.



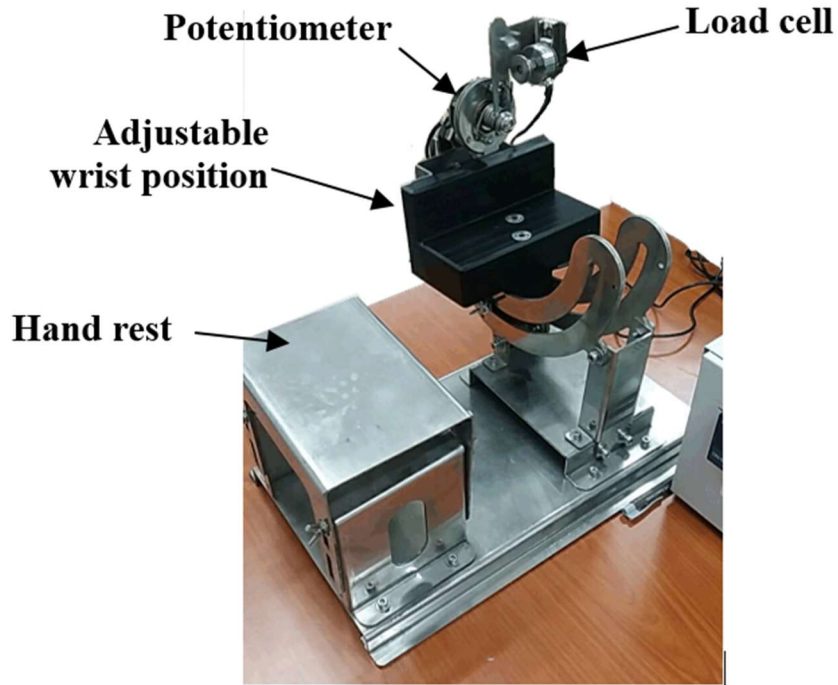


Figure 3.1: Portable Thumb Training System

The hand rest platform was designed to keep the forearm in a resting position, which was essential. During the collecting procedure, the subject's forearm was placed on the platform to minimise unnecessary contraction of the muscles. Muscle contraction during non-exerted force (during relax condition; unwanted contraction) can cause undesired force exerted by the subject during contract condition.

During the data collection procedure, a potentiometer was used on the platform to measure the angle of the subjects' thumbs. Using Simulink (Matlab 2020), Figure 3.2 depicts how the thumb angle's block diagram was developed. An analogue value originating from the potentiometer was fed to the 'Gain 3' block and was converted into voltage form using the formula shown in Equation 1. The analogue input was divided by 1024 as the maximum number of analogues before it was multiplied by 5, which indicates the maximum voltage that the processor (Arduino) can read.

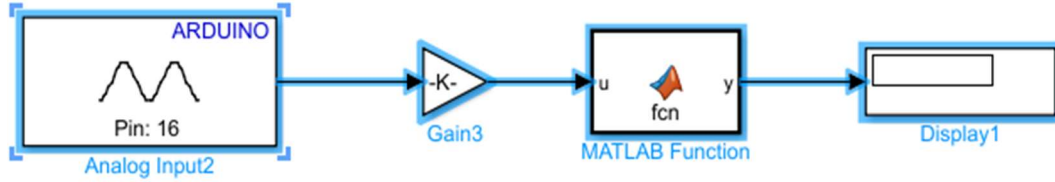


Figure 3.2: Angle block diagram

$$K(\text{digital voltage}) = \text{input} \times \frac{5}{1024} \quad (1)$$

Equation 1: conversion: from analogue to voltage values of load cell signal

After that, the voltage value was passed to Matlab function's block for calibration purposes using "Angle Meter" apps to utilise Equation 2. As shown in Figure 3.3, the thumb attitudes were fixed at zero degrees, thirty degrees, sixty degrees, and ninety degrees and displayed to the users. On the platform, the load cell was screwed based on the angle accordingly.

$$\text{output (angle)} = \text{input (digital voltage)} \times 55.641 + 0.6266 \quad (2)$$

Equation 2: Conversion of voltage to angle

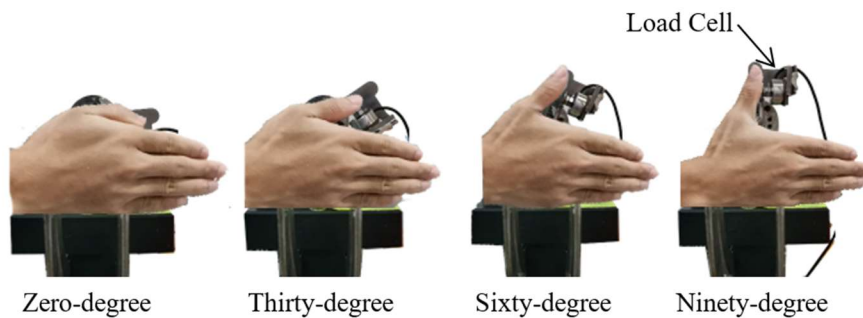


Figure 3.3: Thumb attitudes

A load cell was used to capture the force exerted by the subjects. The forces exerted were constant variables in this experiment and it was controlled by contraction muscles. The contraction muscles to achieve the desired force generated a biopotential signal and the signal was analysed in this experiment to see whether the signal successfully classified the different thumb attitudes. Calibrations of the load cell were conducted using known metal calibration weights which acted as forces applied by the subjects in the real system.

### **3.3 TRAJECTORY**

A dedicated trajectory was designed to guide the subjects in applying dedicated amounts of force on the load cell for the data collection procedure. The trajectory is necessary to standardise the duration and the force applied during the experiments.

Previous researchers used three levels of Maximum Voluntary Contraction (MVC) which are 10%, 30%, and 50% (Jordanić et al., 2017; Rojas-martínez et al., 2012) to study the reactions of different MVCs that affected muscles fatigue. MVC is the maximum contraction that muscles can exert, where the power generated by the activities depends on its amount (Dahlqvist et al., 2018). A study conducted by Rozand et al., (2014) found that the higher the MVC percentage exerted, the faster muscles become fatigued as it takes a longer period for ion in muscle levels to recover. In this case, the highest MVC that can be considered to be applied by the participant is 50% of the maximum force. In contrast, the disadvantage of using lower MVC is that has a low ion value, which results in low amplitude captured by sensors, thus causing readings to be too difficult to be analysed (Barru et al., 2018). It is reflected by 10% MVC. As such, in line with the suggestion by Aranceta-Garza and Conway, (2019), the fixed force to be exerted by the subjects in this study is 30% MVC.

The contraction duration (with the exertion of force) was set to five seconds and eight seconds for relaxation (no force exerted). Relax duration was set to be 1.5 times more than the contract duration in line with an earlier study (Aranceta-Garza and Conway, 2019). The time provided was believed to be enough for muscles to recover the ion lost during the previous contraction procedure before the muscle is ready again for the next contraction procedure. Also, one second was set as a transition time for the subjects to change from relaxing to contracting mode and vice versa. The conditions (contract and relax) were repeated three times in one record to ensure that there was enough sample to be analysed in the next process, and this took approximately 50 seconds per record. The trajectory sample is illustrated in Figure 3.4.

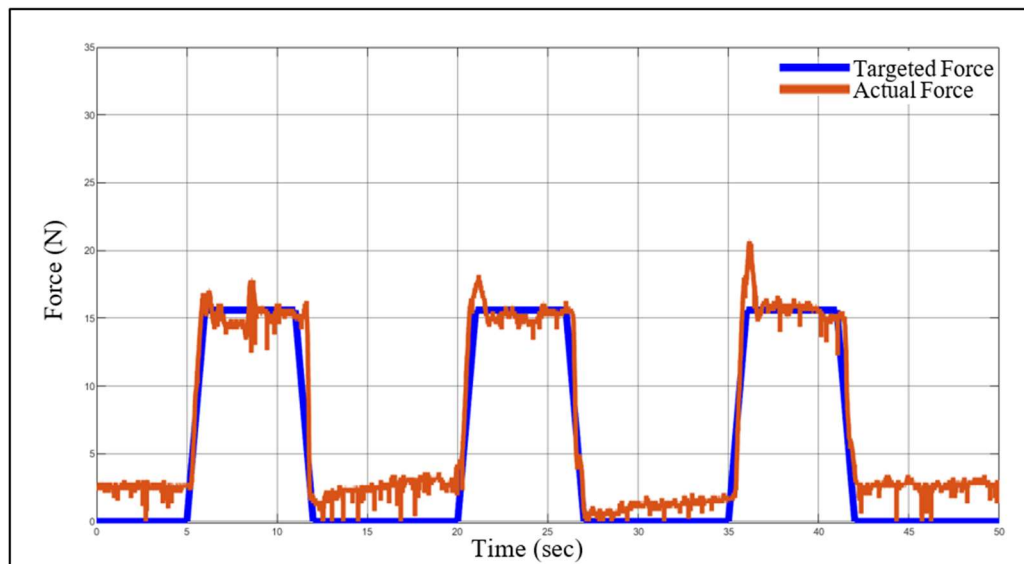


Figure 3.4: Trajectory interface

A Simulink block diagram for developing the dedicated trajectory is shown in Figure 3.5. The block diagram was split into three sections. The first section was the block diagram to capture the analogue signal from the Arduino and convert it into a force unit.

This component included ‘Analog Input 1’, which was set to pin 0 and a display on the block that showed ‘Arduino Pin 14’ as well as two ‘Gain’ blocks labelled ‘Gain 1’ and ‘Gain 2’.

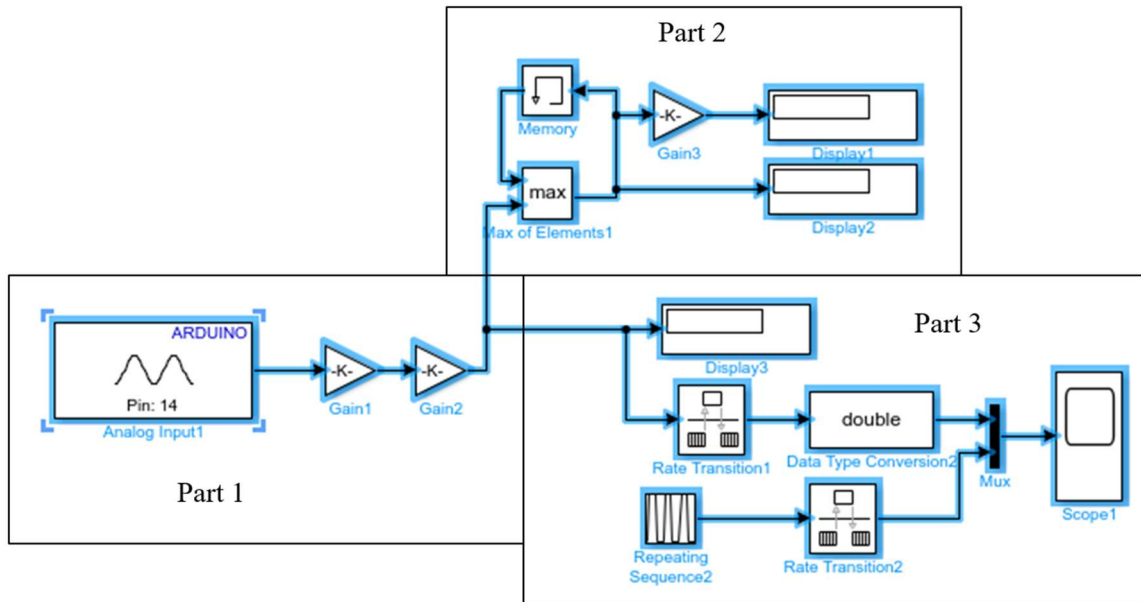


Figure 3.5: Force block diagram

Equation 1 was installed in ‘Gain 1’ as the conversion of the analogue read to a 5V maximum value. The value was then supplied to the ‘Gain 2’ block as the conversion to the value of force (N) using equation 3. In this equation, the input was multiplied by 20, which was the value of ‘m’ (gradient) in the straight-line equation (also known as a straight line’s slope). The value of 20 was fixed based on the output of the calculation straight-line slope during the load cell calibration process. The numbers were then multiplied by 9.80665 which indicated the conversion value from gram to newton before being divided by 5, indicating the maximum voltage value. As a result, the output of the ‘Gain 2’ block was a force with SI units of Newton (N).

$$\text{output}(\text{force exerted}(N)) = \text{input}(\text{digital voltage}) \times 20 \times \frac{9.80665}{5} \quad (3)$$

Equation 3: conversion voltage to force (N)

Part 2 and Part 3 were dedicated to measuring 30% of the MVC applied by the subjects using several blocks such as ‘Max of element’, ‘Memory’, ‘Gain’, and ‘Display’. The force value originated from Part 1 and was fed into a block known as ‘Max of Elements 1’. Using the ‘Memory’ block, the current force value (while imagining the system is running) was compared with an earlier maximum force value saved from the same dataset. The current subject’s maximum force was shown in the ‘Display 2’ block. At the same time, the highest force exerted was the input for the ‘Gain 3’ block. The block (Gain 3) calculated 30% of the maximum force and the result was displayed in the ‘Display 1’ block. The 30% MVC value was set in part three to be used in the actual trajectory during the data collection procedure manually.

Part 3 contains several blocks for generating a trajectory to be used in the data collection procedure. This part includes two ‘Rate Transition’ blocks, one ‘Data Type Conversion’ block, one ‘Repeating Sequence’ block, one ‘Mux’ block and one ‘Scope’ block to display the generated trajectory. The desired graph was created using the ‘Repeating Sequence 2’ block as demonstrated in Figure 3.6. The time intervals were set to 0, 2, 7, 9, and 15. The contraction period began in sec 2 until sec 7 (5 seconds), and then the relaxed period began from sec 7 until sec 15 (8 seconds). This ratio was used in earlier research (Aranceta-Garza and Conway, 2019). The output values began with 0 N at 0 sec, then sec 2 and 7, and the output set differed at this point depending on the 30% MVC. The signal then passed through the ‘Rate Transition 2’ block with an output port sample time of 1/200 together with the current force values from the load cell at the same rate. The selection of this sample time was after trying multiple sample rates. The ‘Rate Transition’

block was necessary to ensure that the transfer rate for both signals was the same to avoid the lagging trajectory displayed in ‘Scope 1’. The output from the ‘Rate Transition 1’ block was then passed to the ‘Data Type Conversion’ block so that the value can be converted into a readable value. ‘Mux’ block was used to combine both live data and generated repeating sequence trajectory for comparison purposes (with double as the data type). ‘Display 3’ then showed the subjects' real-time force exerted.

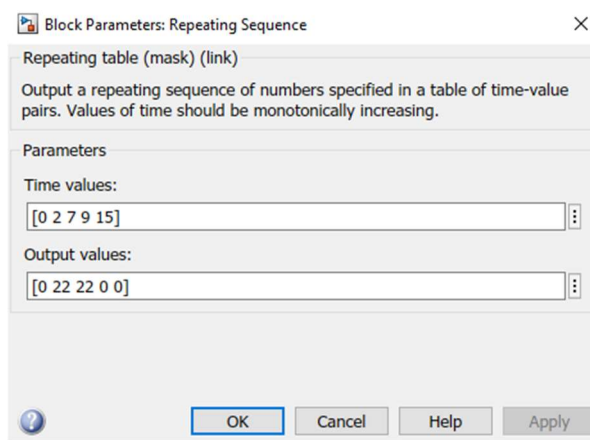


Figure 3.6: Desired graph parameter

### 3.4 DATA COLLECTION PROCEDURE

Figure 3.7 represents the flowchart for the data collection process. This research was approved by the International Islamic University Malaysia (IIUM) Research Ethics Committee (Approval ID: 2020-080) (see Appendix I). The subjects were provided with a consent form (see Appendix II) before the procedure began. The subject's forearm length was then measured using the 25% rule as shown in Figure 3.8 according to a standard

procedure from a previous study by (Aranceta-Garza and Conway, 2019) before proceeding with placement of an HD-sEMG electrodes pad on the subject's forearm.

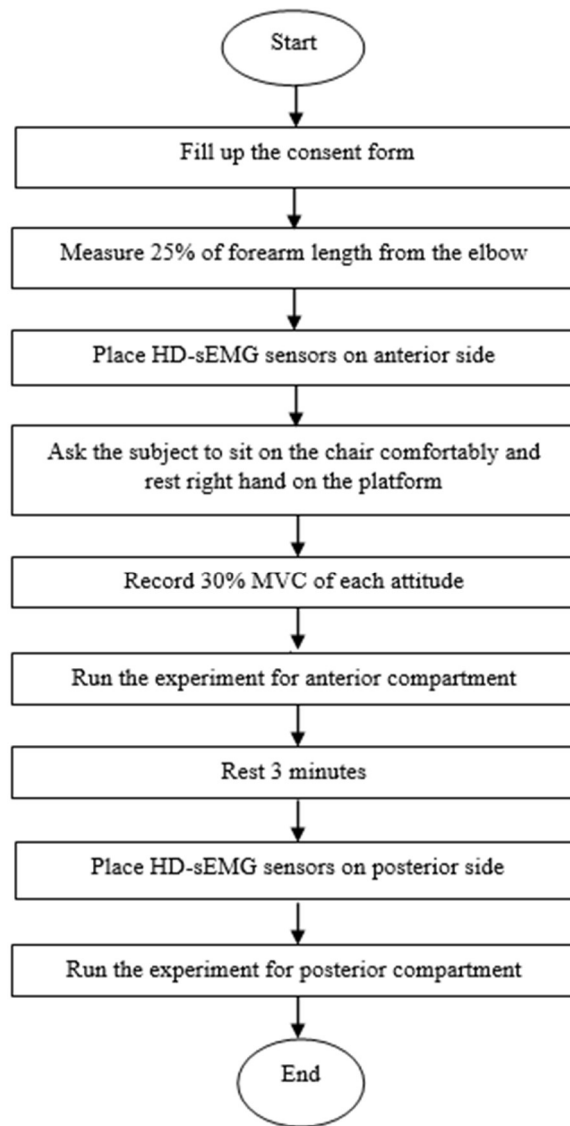


Figure 3.7: Procedures for data collection



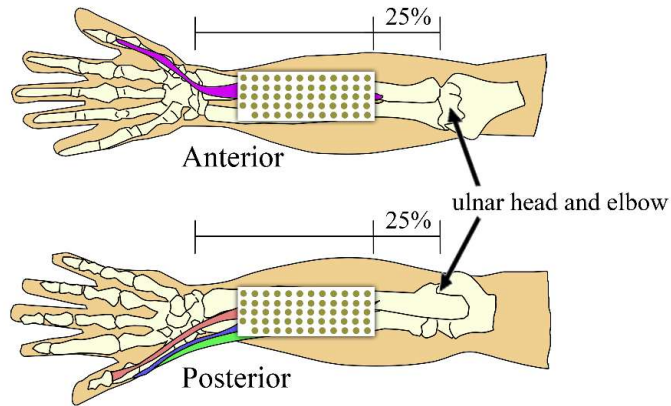


Figure 3.8: Electrode placement standard

The procedure began with the anterior side. First, the electrode was placed on the measured forearm. Then, the subject was asked to sit on a chair facing a dedicated computer screen, while the experimenter adjusted the subject's forearm position on the portable thumb training system as shown in Figure 3.9.

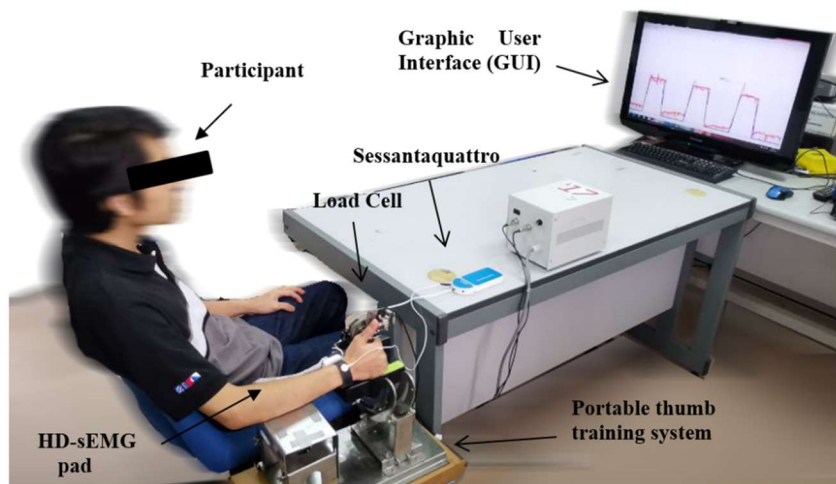


Figure 3.9: Experiment setup to collect the HD-sEMG signals recording

The manipulated thumb attitudes were the thumb angles, namely zero degrees, thirty degrees, sixty degrees, and ninety degrees. The experiment began with the MVC of individual subjects measured using a load cell. The subject was asked to exert his or her maximum thumb force on the load cell before the Simulink automatically calculated 30% of his or her MVC. The 30% MVC again was set by Simulink as the targeted force before being shown through a graphical user interface (GUI) in trajectory form. For repeatability purposes, the subject was asked to apply 30% MVC three times during the procedure.

Subjects were then required to repeat the same procedures three times (three records) for each angle for a total of 12 records for each subject across all angles on one hand side. After completing the anterior side's procedures, the subject rested for three minutes before the posterior side's procedures began. The same rules were applied for the posterior side in which the preparation of the experiment began by placing an electrode at the posterior side of 25% from the ulnar head and elbow. In total, 12 records were collected for the subjects' posterior sides.

### **3.5 HD-sEMG RECORDING SETUP**

A portable biomedical signal amplifier (Model Name: Sessantaquattro) manufactured by OT-Bioelettronica illustrated in Figure 3.10 was used to capture 64 channels of monopolar HD-sEMG signals.



Figure 3.10: Sessantaquattro by OT-Bioelettronica

Data collected from the HD-sEMG patch can be transmitted from an amplifier via Wi-Fi to PCs, tablets, or smartphones or stored on an SD card for long-term acquisition. Different adapters allow the Sessantaquattro connection of electrode matrixes, electrode arrays, or bipolar electrodes. Sessantaquattro can also act as a 64 channel data logger that stores data on a MicroSD card.

The electrode used in this experiment was the GR08MM1305, which is an HD-sEMG electrode pad that has 13 rows and 5 columns grids with an 8 mm inter-electrode distance as illustrated in Figure 3.11. The pad was placed on both sides of the subject's forearm. The electrode required foam to ensure that it could adhere to the forearm. Also, the specific foam used together with this electrode was the KIT08MM1305 (as shown in Figure 3.12), and a special cream known as conductive cream (CC1) was utilised to fill up spaces inside the foam to ensure that the biosignal can be captured by the electrode with minimal noise.



Figure 3.11: HD-sEMG electrode

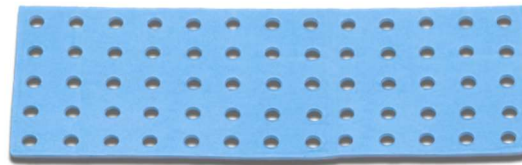


Figure 3.12: HD-sEMG electrode foam

To acquire or process the signals in real-time, a custom application for Sessantaquattro was developed. Alternatively, a freeware software OT BioLab was used to display real-time signals and acquire the Sessantaquattro signals used in this experiment. Before the data acquisition process started, the software settings had to be updated. Figure 3.13 depicts the software setup for this study. Using the GUI of the software, the device was set to Sessantaquattro, and the adapter option was set to AD1x64SE. The adapter option selected (AD1x64SE) was compatible with the plugging of the GR08MM1305 electrode. All the configurations were set under sensor settings. The frequency system was also set to EMG (2000Hz) for the HD-EMG signal as fixed by the manufacturer in the user manual (Manual, n.d.). After everything was set, the data collection procedure could then begin.

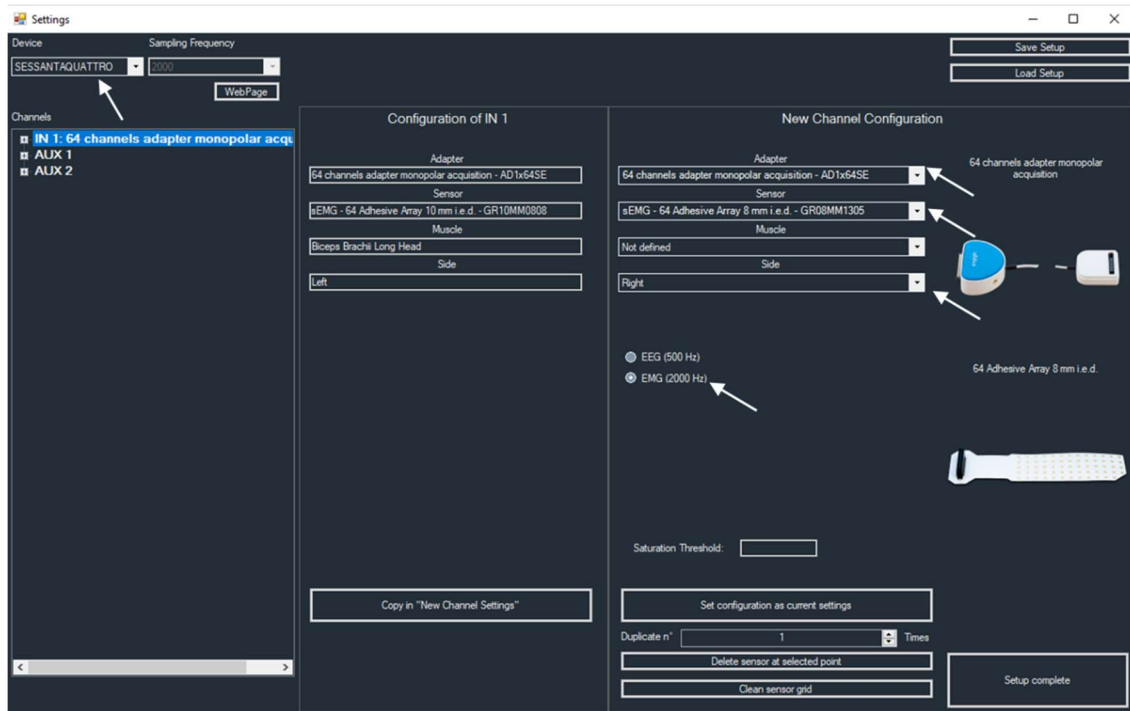


Figure 3.13: HD-sEMG software setting

### 3.6 FEATURE EXTRACTION

In this experiment, there were four features extracted with two from the TD, namely the RMS and MAV or known as Absolute Rectified Value (ARV). These two features are well-known optimal methods to extract signal amplitude (Phinyomark et al., 2013). Despite the previous study's result that the TD has better features in classifying thumb attitude, two FD features were also included in this study, namely MNF and MDF. These two features are the most basic and commonly used in for FD.

The RMS was obtained by calculating the mean value of the EMG signal using Equation 4.

$$RMS = \sqrt{\frac{1}{N} \sum_{k=1}^N |x_k|^2} \quad (4)$$

Equation 4: RMS equation

The ARV feature is an average absolute value of the EMG signal amplitude in segmentation as shown in Equation 5.

$$ARV = \frac{1}{N} \sum_{k=1}^N x_k \quad (5)$$

Equation 5: MAV/ARV equation

in which:

- 'N' is the number of samples per window.
- 'X<sub>k</sub>' is the amplitude of the signal at the input of the amplifier in mV.

MNF is the average frequency of the signal. It is also known as the central frequency (Fc). It is expressed as shown in Equation 6.

$$MNF = \frac{\sum_{i=1}^M f_i P_i}{\sum_{i=1}^M P_i} \quad (6)$$

Equation 6: MNF equation

MDF is the frequency at which the power spectrum density is split into two halves; in other words, MDF is half of the total power as expressed in Equation 7.

$$\text{MDF} = \frac{1}{2} \sum_{i=1}^M P_i \quad (7)$$

Equation 7: MDF equation

in which:

- $f_i$  is the frequency of the spectrum at frequency  $i$ .
- $P_i$  is the power spectrum at frequency  $i$ .
- $M$  is the length of the frequency bin.

### 3.7 SOFTWARE INTERFACE AND DATA EXTRACTION

Software provided by OT BioLab was used to do the pre-processing steps. An example of an offline GUI of the software is shown in Figure 3.14. As demonstrated in the figure, the software is equipped with a ‘Channel List’ column on the left side, next to the signal display known as ‘Tab 1-RawData’. The ‘Tab1-RawData’ displays the pattern of the collected HD-sEMG signal in the loop. This channel was used to visualise and analyse the captured signal to determine whether it is acceptable or not.

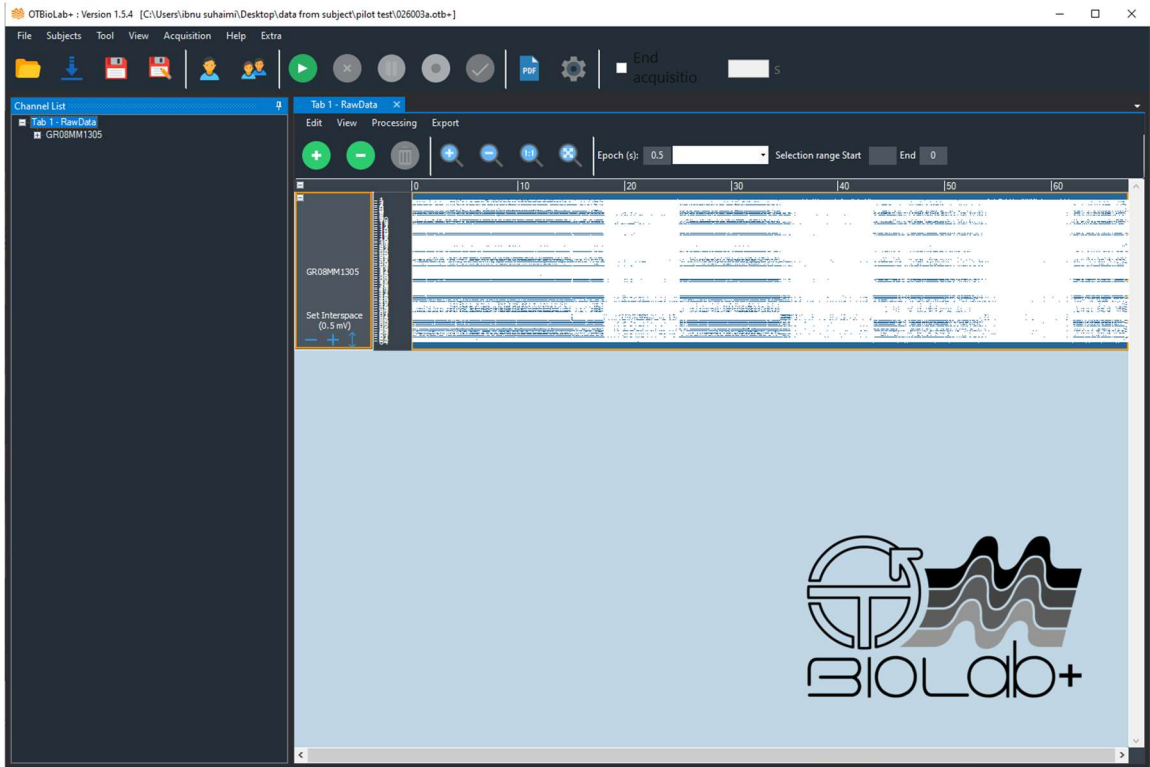


Figure 3.14: OTBioLab data interface

By zooming in on the ‘Tab1-RawData’ graph, Figure 3.15 represents the electrode arrangement of all 64 electrodes (labelled as 1). The amplitude interspace (labelled as 2) was determined by the subject signals, which means that different subjects had different interspaces. In case the differences between the set conditions (contract and relax) were too small, the interspaces were smaller and vice versa. As a result of adjusting the interfaces, the contact (labelled as 3) and the relax (labelled as 4) can now be clearly seen. Based on the trajectory shown in Figure 3.14, as the participants were required to apply force three times in each record for the contact condition, these signals are portrayed in the resulting sample in Figure 3.15.





Figure 3.15: Signal interface details

OT BioLab software also was used to extract the dedicated features. Figure 3.16 depicts the offline processing features selection. As a note, all of the features selected to be analysed in this study were ready to be calculated automatically by the software. These features were labelled as 1 (ARV), 2 (MNF), 3 (MDF), and 4 (RMS).

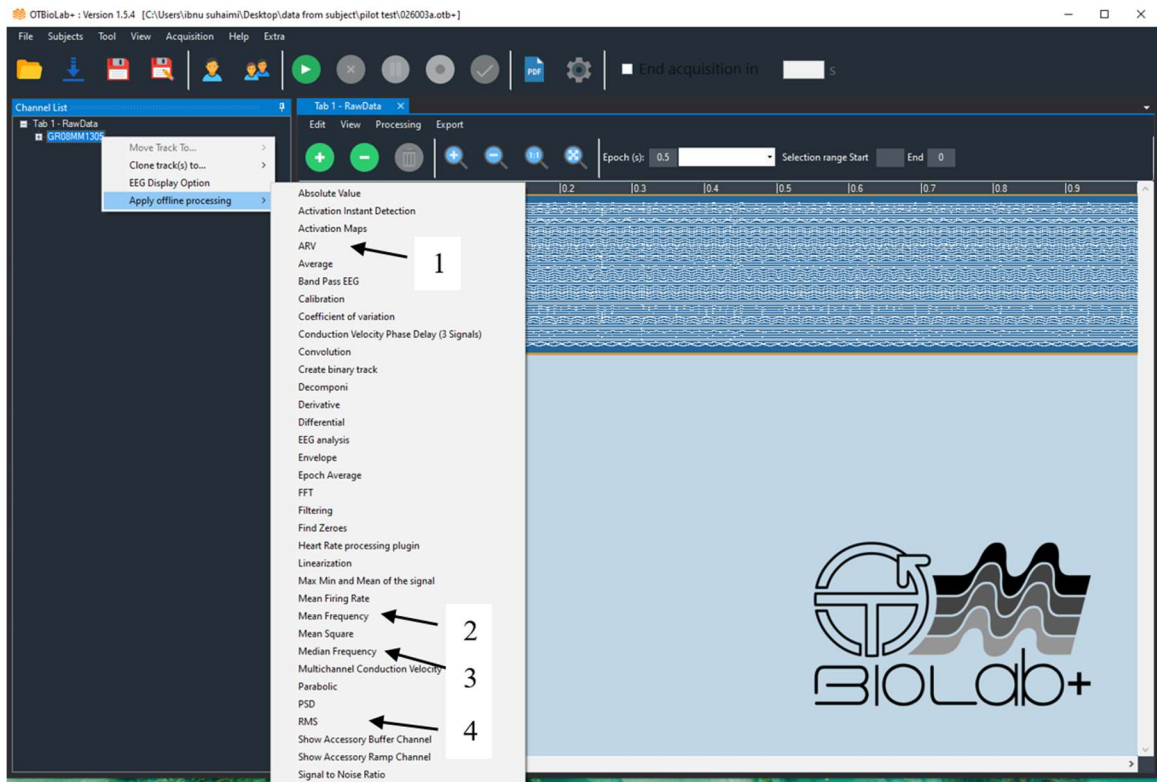


Figure 3.16: Offline processing direction (feature extraction)

Once the interesting feature was selected by the user, a new row of signals will appear below the raw signals as shown in Figure 3.17. The example of a selected feature depicted in the figure is ARV.

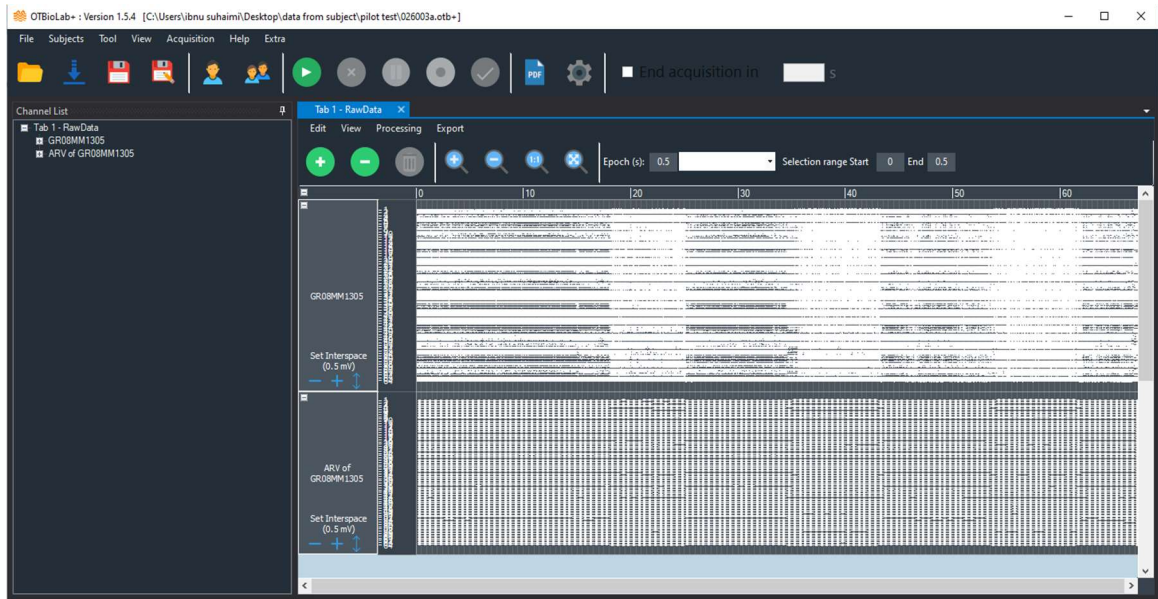


Figure 3.17: Feature extracted interface

Then, the extracted feature can be exported into a variety of file formats, including .mat, .csv, binary, and .wav depending on the demand of the users. While the export data records the entire duration of the data collection process, the data can be filtered to a specific period as shown in Figure 3.18. In the case of this study, the only data of interest to be analysed was during the contract and relax conditions. As such, the rest of the data were ignored. These selected data were later exported into a file for the following processing steps.

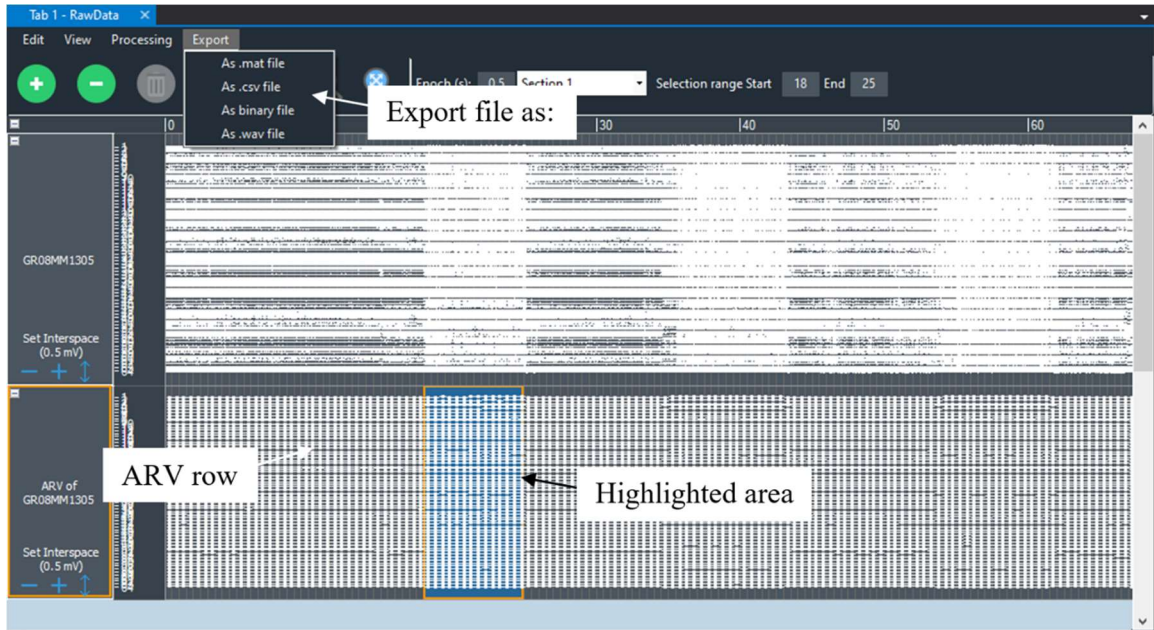


Figure 3.18: Feature extracted interface details and export direction

### 3.8 NORMALISATION DATA

Since the HD-sEMG signals recorded from each subject were unique and there were also variations of the 30% MVC value recorded among subjects, there was a need for the data to be normalised in the next pre-processing steps. Normalisation is important due to inter-day and inter-subject variations of the HD-sEMG signals (Bashford et al., 2020). Mathematically, the normalisation of the HD-sEMG can be expressed as shown in Equation (3).

$$\frac{n}{\bar{x}} \times 100\% \quad (8)$$

Equation 8: Normalisation equation

where:

‘ $\bar{x}$ ’ is the average of all normalised data values

‘ $n$ ’ is the data from the  $n^{\text{th}}$  electrode out of 64 electrodes

To normalise the data, first, the average of each feature data set of all electrodes was calculated ( $\bar{x}$ ). Then, the RMS or ARV value of the specific electrode ( $n$ ) was divided by the  $\bar{x}$  before being multiplied by 100 to scale up the normalised values.

### 3.9 CLASSIFIER

Classification is an important step in identifying patterns of HD-sEMG signals that correspond to specific thumb muscle force exertion magnitudes and postures. In this study, the pre-processed data were classified using machine and deep learning classification learner app in Matlab R2020 (The Mathworks, Natick, MA).

Using trial and error method, the cross-validation value was set as five folds after a few attempts at different settings from 1 up to 10. This implies that all input data from the HD-sEMG signal were divided into five groups automatically using a ratio of 1:4 (e.g., Group 1 for testing and four other groups, Group 2 to 5, for training). After the first classification iteration, the testing group was rotated (Group 2 was now meant for testing while Group 1 and Group 3 to 5 were used for training). The whole classification process took five times, indicating the five folds, and all five groups were used for testing. The result displayed is the mean of the overall five classification results (Frank et al., 2010). The training and testing data sets were randomly selected by the app.

The classifiers selected in this study were LDA, SVM, and KNN, in addition to one random classifier, which was the TREE-based classifier. For the KNN classifier, the value of the variable  $K$  which indicated the count of the nearest neighbours can be manipulated based on the data. In this study, the  $K$  value was set to 1 because it produced the highest correctly classified instances after comparing to other  $K$  values between 1 to 10. The selection of these three classifiers namely LDA, SVM, and KNN was because there were commonly used classifiers in a previous study that focused on replicating hand posture in a prosthetic hand study that produced a highly accurate result. The premier study of this research used the Weka machine learning algorithm, and the TREE-based classifier produced high accuracy; thus, the TREE-based classifier was included in the actual study.

Machine learning classification was carried out such that the inputs to the machine learning algorithm were HD-sEMG data that were collected from the 64 electrodes placed on the forearm anterior and posterior muscles and the outputs were the corresponding thumb postures at zero degrees (at rest and contract), thirty degrees (at rest and contract), sixty degrees (at rest and contract) and ninety degrees (at rest and contract), which were denoted as class A, B, C, D, E, F and H respectively as shown in Table 3.1.

Table 3.1 Denotation of Thumb Posture Classes

Thumb Posture	Class
Zero Degrees (contract)	A
Thirty Degrees (contract)	B
Sixty Degrees (contract)	C
Ninety Degrees (contract)	D
Zero Degrees (at rest)	E
Thirty Degrees (at rest)	F
Sixty Degrees (at rest)	G
Ninety Degrees (at rest)	H

Figure 3.19 depicts the classifier's basic configuration. In this experiment, the response option must be set to angle, which was the targeted class. There were eight distinct classes, each with four angles (zero degrees, thirty degrees, sixty degrees, and ninety degrees) and two different conditions (contract and relax). Data that did not include predictors were unmarked, as condition, sub, and trial data were excluded in this study.

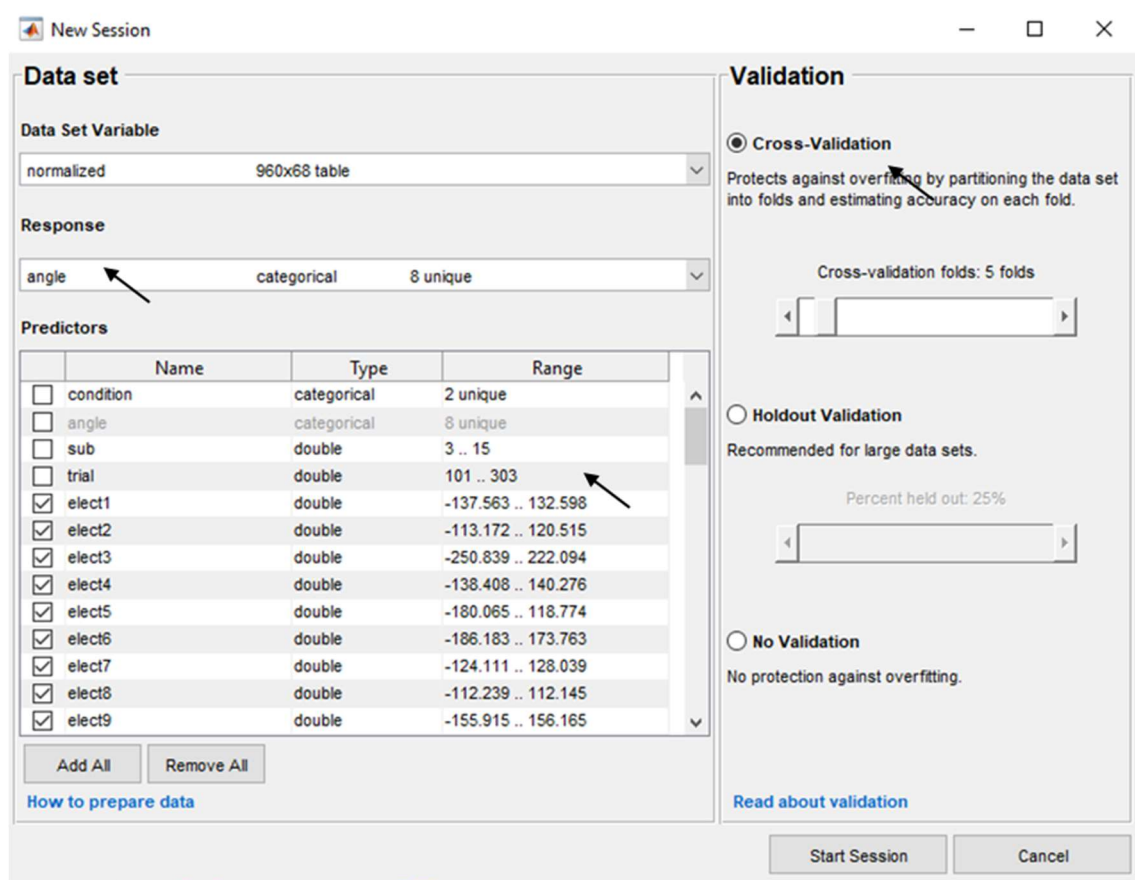


Figure 3.19: Classifier setting

### **3.10 SUMMARY**

To sum, this chapter presented the experimental set ups for data collection and data analysis processes. Four different attitudes were fixed in collecting dedicated HD-sEMG signals from extrinsic muscles at zero degrees, thirty degrees, sixty degrees, and ninety degrees using a developed thumb training platform. Two features from the TD family (RMS and ARV) and two from the FD (MNF and MDF) were chosen to be extracted. Using Matlab R2020, there were four chosen classifiers selected, namely LDA, SVM, and KNN, as well as one random TREE-based, to classify the collected data. The outcomes of the study are discussed in the following chapter.



## **CHAPTER FOUR**

### **RESULT AND DISCUSSION**

#### **4.1 INTRODUCTION**

In this chapter, the entire results starting from the data collection process up to the classification process are discussed. The first result to be elaborated is the amount of force exerted by the subjects, followed by the comparison between RAW and normalised data based on the selected features and classifiers. These are the two features from TD (ARV and RMS) and FD (mean and median) using four different classifiers namely LDA, SVM, KNN, and TREE-based. After that, the outcomes from the best feature and classifier (with the highest accuracy) applied to both hand sides (anterior and posterior) are discussed in finalising the study results.

#### **4.2 PARTICIPANT**

A total of 17 subjects (12 males, 5 females; age  $26.5 \pm 3.5$  years) took part in this experiment and were purposely selected among International Islamic University Malaysia students with no history of hand injury. Thirty percent of MVC force of each attitude (angle) was recorded as tabulated in Table 4.1.

Table 4.1: Result of 30% MVC force

Subject ID	Gender	Age	30% MVC (N)			
			Zero degrees	Thirty degrees	Sixty degrees	Ninety degrees
1	Male	26	11.84	11.49	10.57	18.1
2	Male	26	8.56	9.538	12.35	19.31
3	Male	30	8.15	10.24	14.48	18.44
4	Male	27	7.97	12.28	12.17	14.87
5	Male	25	7.68	11.02	14.7	16.99
6	Male	24	8.26	9.24	10.9	13.78
7	Male	25	7.89	11.23	12.5	17.56
8	Male	26	6.98	8.21	10.35	11.68
9	Male	26	7.84	7.98	9.84	10.96
10	Male	25	8.45	9.42	12.82	12.35
11	Male	28	7.87	7.98	9.93	10.67
12	Male	27	7.46	8.38	11.87	12.91
13	Female	25	7.05	6.71	6.01	16.02
14	Female	30	2.39	5.1	5.559	6.996
15	Female	25	6.42	6.43	6.938	8.547
16	Female	27	5.48	5.89	6.53	7.03
17	Female	26	6.67	6.86	7.54	7.81

It is clear from these findings that the magnitude of thumb force exerted by the subjects varied significantly. The 30% MVC varied depending on the angular position of the thumb, which was also observed. For example, the value of 30% MVC at the ninety-degree position was generally higher than the value of 30% MVC at the zero-degree position (see Figure 4.1).

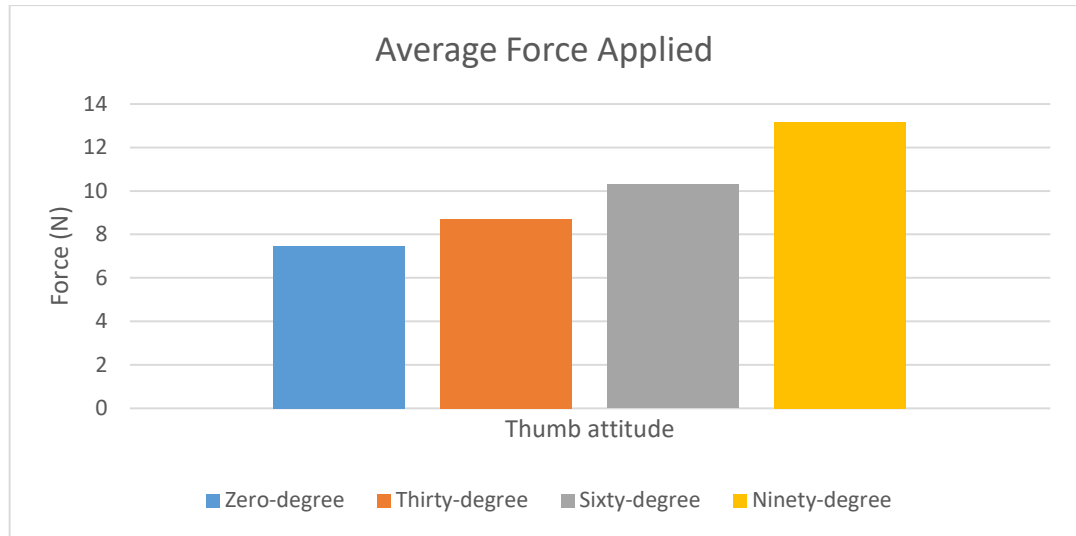


Figure 4.1: Average force applied at 30% MVC in each posture

### 4.3 STATISTICAL ANALYSIS

Statistical analysis was run using Statistical Package for the Social Sciences (SPSS)<sup>1</sup> software to test (i) correlation between the electrodes and (ii) interaction effect of hand sides, features, conditions, and angle of the thumbs on the HD-sEMG (force) data captured by the electrodes.

#### 4.3.1 CORRELATION ANALYSIS

A 2-tailed Pearson product-moment correlation was run to determine the relationship between the HD-sEMG electrode readings (electrode 1 to electrode 64). As results, there were strong positive correlations within the electrodes, which were statistically significant, ( $r \geq 0.859$ ,  $n = 3840$ ,  $p < 0.01$ )

<sup>1</sup> <https://www.ibm.com/products/spss-statistics>

### 4.3.2 INTERACTION EFFECT

A Multivariate Analysis of Variance (MANOVA) was run to test the interaction effect of hand sides (anterior vs posterior), features (ARV vs RMS), conditions (contract vs relax), and angle of the thumbs (zero degrees vs thirty degrees vs sixty degrees vs ninety degrees) on the HD-sEMG readings. The result indicated a significant interaction effect of the independent variables on the dependent variables with *Wilks'  $\Lambda$*  = 0.930,  $F(192,11229) = 1.427$ ,  $p < 0.010$ , partial  $\eta^2 = 0.024$ . The hand sides, features, conditions, and angle of the thumbs contributed to the force readings captured by the HD-sEMG.

### 4.4 HD-sEMG MAP

The collected signals from the patch can be visualised based on colour using a map. At the sampling rate of 2000 Hz, HD-sEMG activation maps were generated based on RMS and ARV features which were extracted from the 64 channels of HD-sEMG. Figure 4.2 displays the HD-sEMG activation maps for each posture obtained from one of the subjects (randomly chosen: Subject 6).

The HD-sEMG activation maps indicate regions of muscles that had high levels of biopotential activations during a specific thumb force exertion and the regions of muscles that have lower biopotential activations. Regions that had higher levels of muscle activations are represented by a dark red colour whereas regions that have lower levels of muscle activations are represented by light blue and dark blue colours. It can be observed from Figure 4.2 that the variation in the colours presented on the HD-sEMG activation map depends on both the feature extraction method used (ARV or RMS) and the thumb posture (zero degrees, thirty degrees, sixty degrees and ninety degrees).

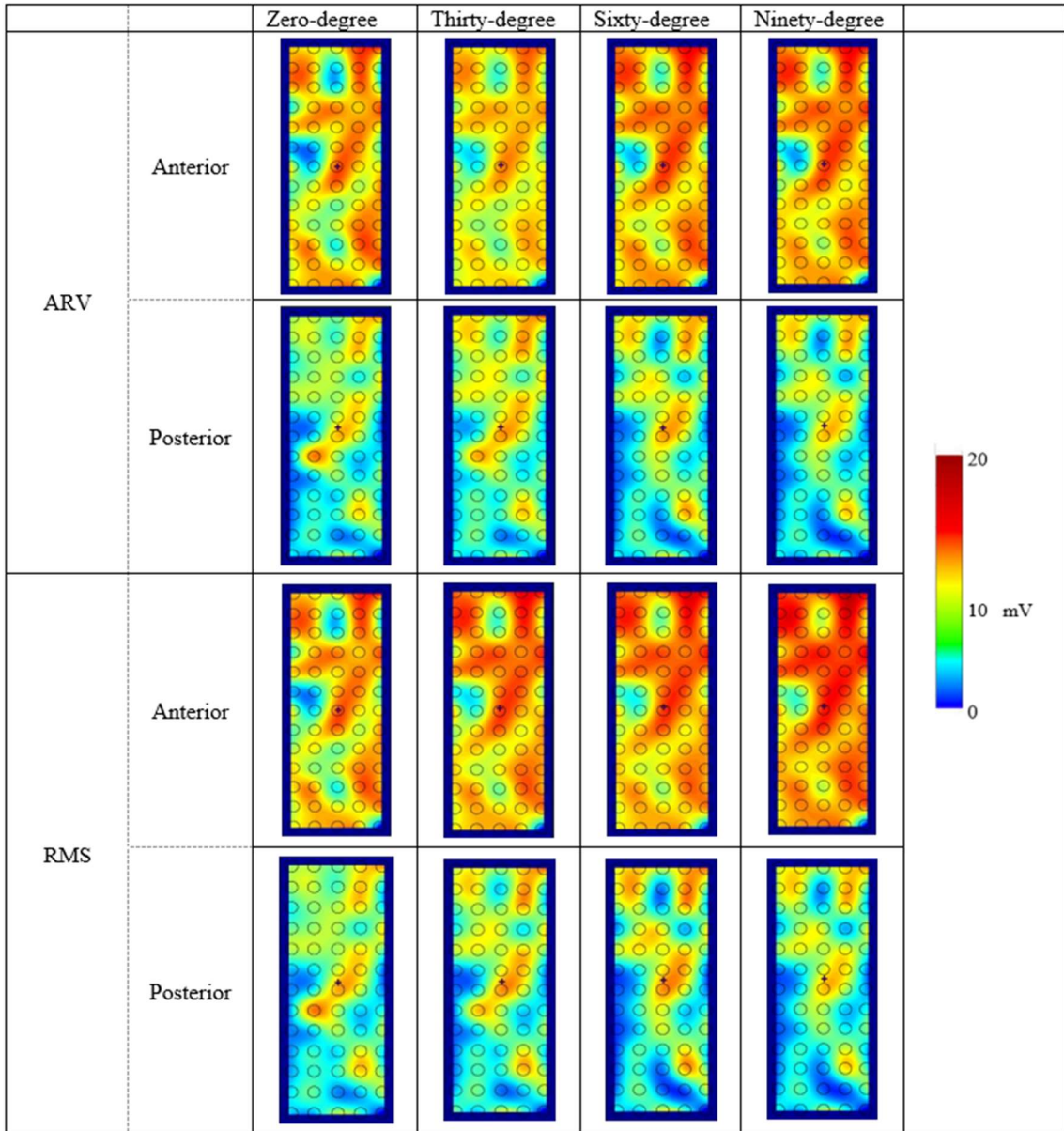


Figure 4.2: HD-sEMG activation maps at each thumb posture for Subject 6 using ARV and RMS features

As a result, it can be observed that the amplitude of both RMS and ARV values of the signal measured from the forearm anterior side was higher compared to the posterior side for all the postures based on colour density. For the posterior side, the amplitude of

both the RMS and ARV became lower as the angle of the thumb increased. On the other hand, on the anterior side, the RMS and ARV amplitudes became higher as the angle of the thumb increased. It was also observed that the RMS feature generated higher amplitudes as compared to the ARV feature in general and this was observed in the EMG activation maps.

#### **4.5 THE BEST FEATURES AND CLASSIFIERS**

The focus of this chapter is to analyse and discuss the result of different features and classifiers. The best feature and classifier are finalised toward the end of this chapter and were used as the main feature and classifier of the experiment. It is important to mention here that the result discussed in this part comprises the features and classifier using the anterior hand side data only. The reasoned selection of the data from this part of the forearm is because the muscle (Flexor Pollicis longus) is one of the preserved muscles for the transradial amputee and the signal is used to control the prosthetic hand (Pierrie et al., 2019).

The data in Table 4.2. displays the classification results for two sets of data. The RAW data as well as normalised data are included in the table. The features for each set were MNF, MDF, ARV, and RMS. In comparison, the normalised process improved the classification result for various classifiers of different features.

Table 4.2: Classification result for RAW and normalised data for each classifier

Data	Domain	Feature	Classifier			
			LDA	SVM	KNN	TREE
			Correctly classified instances (%)	Correctly classified instances (%)	Correctly classified instances (%)	Correctly classified instances (%)
RAW	Frequency	MNF	72.5	69.2	74.8	56.9
		MDF	47.6	60.8	69	60.1
	Time	ARV	30.3	71.7	83.8	70.1
		RMS	88.2	73.2	82.4	70.1
Normalized	Frequency	MNF	80.2	77.5	81.8	73.6
		MDF	56.8	62.4	78.8	70.1
	Time	ARV	97.1	85.7	94.0	86.1
		RMS	96.4	87.8	95.0	86.3

The highest increment correctly classified instances were from the ARV feature classified using the LDA classifier from 30.3% up to 97.1%. The increment made it the highest correctly classified instance followed by the result of the RMS feature using the same classifier (LDA) with 96.4%. Meanwhile, the lowest correctly classified instances for TD of normalised data was the result for ARV feature classified using the SVM classifier with 85.7%.

For the FD, the MNF data classified using the KNN classifier classified the highest accuracy with 81.8% accuracy followed by data of the same feature (MNF) classified using the LDA classifier with 80.2% accuracy. The lowest accuracy was the result for MDF data feature classified using the LDA classifier, with 56.8% correctly classified instances and

followed by the same data classified using the SVM classifier with 62.4% correctly classified instances. These two data sets' results were the only results with less than 70% correctly classified instances of all the results.

Further analysis was done to obtain the accuracy of classification depending on the domain and classifier used on the normalised data.

Table 4.3: Average correctly classified classification for each domain and classifier for normalised data (%)

Domain	Feature	The average classification result from each domain and classifier				The average percentage for each domain
		LDA	SVM	KNN	TREE	
		Correctly classified instances (%)	Correctly classified instances (%)	Correctly classified instances (%)	Correctly classified instances (%)	
Frequency	MNF	68.5	70.0	80.3	71.9	72.7%
	MDF					
Time	ARV	96.8	86.8	94.5	86.2	91.1%
	RMS					
Average percentage for each classifier		82.6%	78.4%	87.4%	79.0%	



Table 4.3 depicts the average of the results for each classifier and domain. KNN recorded the highest average correctly classified instances with 87.4% followed by the LDA classifier with 82.6% correctly classified instances. The percentages for SVM and TREE were less than 80%. As such, it can be deduced that the best classifiers to be used as a preliminary option were the LDA and KNN classifiers.

Additionally, based on the dataset domain, the average TD result of 91.1% correctly classified instances was 18.4% higher than the average FD result of 72.7% correctly classified instances. This percentage demonstrates that TD has a better data set for classification than the FD. The result is also in line with the study conducted by Siddiqi and Sidek (Siddiqi & Sidek, 2016), which concluded that TD analysis yielded higher accuracy in distinguishing different finger postures compared to FD analysis.

TD features and two classifiers namely LDA and KNN had the highest percentage of correctly classified, and the next analysis focuses on these setups. The same setup was applied to the posterior side data, and both results are constructed in Table 4.4.

Table 4.4: Both hand side results for classifier LDA and KNN

Hand side	Feature	Classifier	
		LDA	kNN
		Accuracy (%)	
Anterior	ARV	97.1	94.0
	RMS	96.4	95.0
Posterior	ARV	96.6	98.2
	RMS	96.5	97.8
Average accuracy for each classifier		96.7%	96.3%

KNN scored the highest classification accuracy for the posterior side on average (98%), but for the anterior side, this classifier had lower average accuracy (94.5%). Interestingly, the LDA classifier showed a consistent result for both sides with the highest accuracy recorded from the anterior side for ARV feature with 97.1% and the lowest correctly classified instances on the same hand side (anterior) for RMS feature with 96.4%.

Based on the classifier, on average, LDA had higher correctly classified instances with 96.7% than KNN (with 96.3%). As such, the final decision was to use these TD features (ARV and RMS) with LDA as the classifier for further analysis.

## 4.6 DETAILS OF THE BEST CLASSIFICATION RESULT

Focusing on LDA, inputs for the classifier consisted of TD features (ARV and RMS) and a combination (ARV-RMS) from both hand sides (anterior and posterior); their combination (anterior-posterior) was further analyzed using a confusion matrix. Figure 4.3 demonstrates the percentage of correctly classified instances for each set of data via a bar chart for comparison purposes.

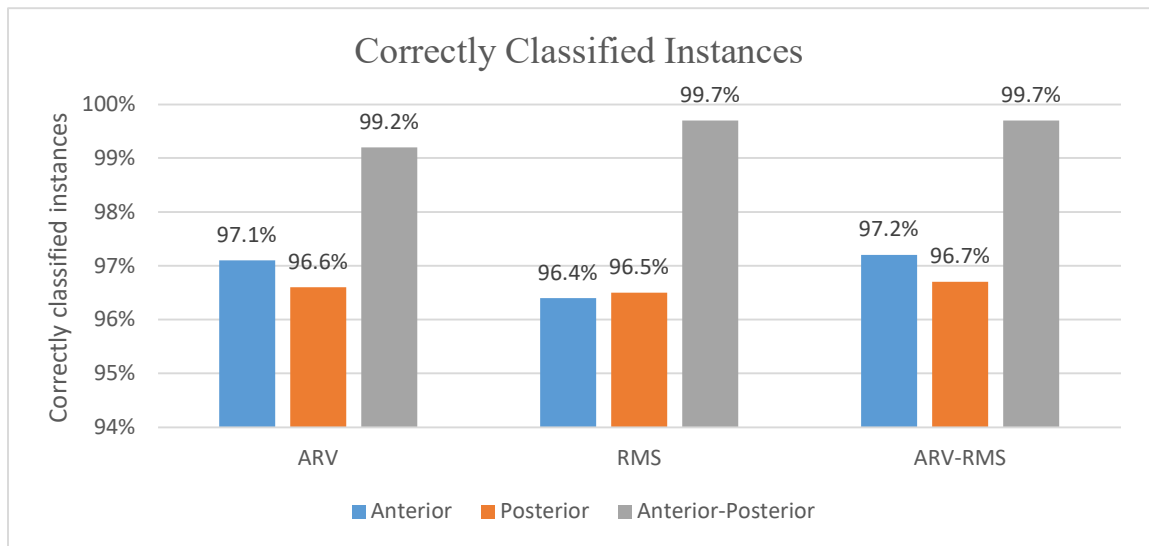


Figure 4.3 Summary of correctly classified instances for ARV, RMS and their combinations based on hand sides

Overall, features extracted from the HD-sEMG yielded more than 96% correctly classified instances for each data set. Using the RMS values, the forearm posterior side (orange bar with label RMS) recorded 96.5% correctly classified instances while the forearm anterior side (the blue bar with label RMS) yielded 96.4% correctly classified instances. The result showed that the data from the forearm posterior had a better-classified

percentage compared to the forearm anterior. These findings coincide with results from a previous study that used the same feature. The study by Aranceta-Garza and Conway, (2019) show result of 94.85% for anterior and 97.00% for posterior which reveals that data from the forearm posterior side resulted in a higher number of correctly classified instances compared to the forearm anterior side for the classification of thumb postures. However, a different pattern was seen in the result for the ARV feature, where the anterior had a better percentage with 97.1% and 96.6% for the forearm posterior.

Classification using a combination of data collected from both the forearm anterior and posterior sides was also carried out. The combination of data from both hand sides utilised 64 electrodes on the forearm anterior and 64 electrodes on the forearm posterior, resulting in a total data collected from 128 electrodes. The results of this combined approach showed a higher percentage of correctly classified instances compared to using data obtained from either the forearm anterior or forearm posterior only. In this combined approach, using the ARV feature results yielded a percentage of 99.2% correctly classified instances whereas using the RMS feature resulted in a slightly higher percentage of 99.7% correctly classified instances. The result shows that the RMS feature had better data in classifying different classes (thumb posture and condition) compared to ARV when both hand-side data are combined.

An additional analysis was also carried out which combined both the ARV and RMS features collected from both the HD-sEMG from the forearm anterior and forearm posterior. This was motivated by a previous study by Siddiqi and Sidek (Siddiqi & Sidek, 2016), which revealed that the percentage of correctly classified instances had increased significantly. The combination of ARV and RMS features together with both forearm anterior and forearm posterior data resulted in a high percentage of correctly classified instances of 99.7%, the same result as using the RMS for both forearm anterior and forearm posterior data. The next discussion will focus on these two data set results which combines

ARV and RMS features of both forearm anterior and forearm posterior with the RMS for both forearm anterior and forearm posterior data.

#### 4.7 CONFUSION MATRIX AND AVERAGE EACH CONDITION

The next analysis was done to investigate the characteristics of the two highest correctly classified instances (RMS and combination feature: ARV-RMS as the features and anterior-posterior as the hand side) found earlier in Figure 4.3. Table 4.5 and Table 4.6 show the confusion matrices for the features respectively. In Table 4.5, the extracted feature was RMS while in Table 4.6, a combination of both the ARV and RMS features was extracted and used as inputs for the classification.

Table 4.5: Confusion matrix for RMS data from the anterior and posterior hand sides.

lass	A	B	C	D	E	F	G	H	Accuracy (%)
A=zero_relax	119		1						99.2
B=zero_contract		119		1					99.2
C=thirty_relax			120						100.0
D=thirty_contract				119		1			99.2
E=sixty_relax					120				100.0
F=sixty_contract						120			100.0
G=ninety_relax							120		100.0
H=ninety_contract								120	100.0
Precision (%)	100.0	100.0	99.2	99.2	100.0	99.2	100.0	100.0	

Table 4.6: Confusion matrix for ARV-RMS data from the anterior and posterior sides.

Class	A	B	C	D	E	F	G	H	Accuracy(%)
A=zero_relax	240								100.0
B=zero_contract		240							100.0
C=thirty_relax			240						100.0
D=thirty_contract				239		1			99.6
E=sixty_relax					239		1		99.6
F=sixty_contract				1		238		1	99.2
G=ninety_relax							240		100.0
H=ninety_contract						1		239	99.6
Precision (%)	100.0	100.0	100.0	99.6	100.0	99.2	99.6	99.6	

Table 4.5 is the result of the RMS data feature of both hand sides (anterior-posterior). Most of the classes were successfully classified except for three classes namely A, B, and D. Misclassification occurred during the classification of zero-degree classes (A and B) with one incorrectly classified as class thirty degrees accordingly (class C and D). Meanwhile, class D had one data incorrectly classified as class F.

In Table 4.6, the number of classified data in this confusion matrix was doubled and enlarged the data up to 240 data via a combination feature where there were 120 data for each feature. There were four classes with an accuracy of 100% (240 data correctly classified), namely class A, B, C, and G. The lowest accuracy with 99.2% was class F with 238 data correctly classified and there were two data incorrectly classified as class D and H each. The other three classes, namely D, E, and H, had 239 data correctly classified with one incorrectly classified.

From both the confusion matrices presented in Table 4.5 and Table 4.6, it can be observed that overall, regardless of the features used, the algorithm accurately classified all the data as their actual class for two classes (C and G) for 100% accuracy and three classes (A, B, and E) for 100% precision. Also, in Table 4.5, it can be seen that there were three incorrectly classified instances out of 960 (99.7%) whereas in Table 4.6, there were five incorrectly classified instances out of 1920 (99.7%).

Table 4.7 summarises the percentages of the two highest accuracy data. Both were the result of a combination of both hand side data with different features (RMS and ARV-RMS).

Table 4.7: Classification results for anterior-posterior hand sides

Feature	Class	Accuracy (%)	Precision (%)
RMS	A=zero_relax	99.2	100.0
	B=zero_contract	99.2	100.0
	C=thirty_relax	100.0	99.2
	D=thirty_contract	99.2	99.2
	E=sixty_relax	100.0	100.0
	F=sixty_contract	100.0	99.2
	G=ninety_relax	100.0	100.0
	H=ninety_contract	100.0	100.0
ARV- RMS	A=zero_relax	100.0	100.0
	B=zero_contract	100.0	100.0
	C=thirty_relax	100.0	100.0
	D=thirty_contract	99.6	99.6
	E=sixty_relax	99.6	100.0
	F=sixty_contract	99.2	99.2
	G=ninety_relax	100.0	99.6
	H=ninety_contract	99.6	99.6

The RMS feature had five classes with 100% correctly classified instances, which were E, F, G, H, and C compared to four classes for the ARV-RMS feature, namely A, B, C, and G. Additionally, five of the classes were classified as 100% precise for RMS feature and four classes for ARV-RMS features. Overall, the RMS feature had 100% accuracy and higher precision than ARV-RMS.

Table 4.8 summarises the average result of conditions (contract and relax) and attitudes (thumb angles) for both features using anterior and posterior hand side data. For RMS, the average correctly classified for relax condition showed 99.8% accuracy and 99.6% for contract condition. From the manipulated variable perspective which was the thumb attitudes, sixty-degree and ninety-degree angles scored 100% accuracy. The attitude of zero degrees resulted in the lowest accuracy with 99.2%.

Moving on to the ARV-RMS feature, the correct classification for the relaxed condition showed 99.9%, while for the contract condition, it showed 99.6% correct classification. For the different attitudes, the only one attitude with 100% correct classification was zero degrees. Other than that, the attitude of sixty degrees was the lowest correctly classified for this data with 99.4%. Besides that, there were two attitudes with 99.8% correct classification, namely thirty degrees and ninety degrees.



Table 4.8: Summary of correctly classified instances based on conditions and attitudes

Features	Condition		Attitudes			
	Relax	Contract	Zero degrees	Thirty degrees	Sixty degrees	Ninety degrees
RMS	99.8 %	99.6 %	99.2 %	99.6 %	100.0 %	100.0 %
	99.7 %		99.7 %			
RMS-ARV	99.9 %	99.6 %	100.0 %	99.8 %	99.4 %	99.8 %
	99.75 %		99.75 %			

#### 4.8 VALIDATION RESULT

For validation, the process focuses on the RMS data set on both sides and implement a 60% training, 20% testing, and 20% testing ratio. This process employs the trainlm training function with 3 hidden layers.

Table 4.9 is confusion matrix for training data set. The results show that there is no misclassification in any of the classes and resultant for 100% for accuracy and precision.

For the testing data set the result shown in Table 4.10. Most of the classes were successfully classified except for two classes namely B and D. Misclassification occurred during the classification of zero-degree contract (class B) with one incorrectly classified as class thirty degrees relax (class C). Meanwhile, class D had one data incorrectly classified as class C.

The confusion matrix for validation data set is shown in table 4.11. Majority of the classes successfully classified for each class except for class A. For the class A they are

one data misclassified as class D and the accuracy for class A is 95.8% and precision class D down to 96.3%.

Table 4.12 is result for all data set and the number of classified data in this confusion matrix total 120 each class. There were six classes with an accuracy of 100% (120 data correctly classified), namely class B, D, E, F, G and H. Two classes do not achieve 100% with 99.2% and 98.3% for class A and B accordingly. The final accuracy is 99.7% and the result align with result classified using classifier LDA.

Table 4.9: Confusion matrix for training data set.

Class	A	B	C	D	E	F	G	H	Accuracy (%)
A=zero_relax	73								100.0
B=zero_contract		72							100.0
C=thirty_relax			76						100.0
D=thirty_contract				76					100.0
E=sixty_relax					72				100.0
F=sixty_contract						69			100.0
G=ninety_relax							70		100.0
H=ninety_contract								68	100.0
Precision (%)	100.0	100.0	100.0	100.0	100.0	100.0	100.0	100.0	

Table 4.10: Confusion matrix for testing data set.

Class	A	B	C	D	E	F	G	H	Accuracy (%)
A=zero_relax	23								100.0
B=zero_contract		27	1						96.4
C=thirty_relax			20						89.1
D=thirty_contract			1	18					94.7
E=sixty_relax					24				100.0
F=sixty_contract						27			100.0
G=ninety_relax							27		100.0
H=ninety_contract								24	100.0

Precision (%)	100.0	100	89.1	100	100.0	100.0	100.0	100.0
---------------	-------	-----	------	-----	-------	-------	-------	-------

Table 4.11: Confusion matrix for validation data set.

Class	A	B	C	D	E	F	G	H	Accuracy (%)
A=zero_relax	23			1					95.8
B=zero_contract		21							100.0
C=thirty_relax			22						100.0
D=thirty_contract				26					100.0
E=sixty_relax					24				100.0
F=sixty_contract						24			100.0
G=ninety_relax							23		100.0
H=ninety_contract								28	100.0

Precision (%)	100.0	100.0	100.0	96.3	100.0	100.0	100.0	100.0
---------------	-------	-------	-------	------	-------	-------	-------	-------

Table 4.12: Confusion matrix for all data set.

Class	A	B	C	D	E	F	G	H	Accuracy (%)
A=zero_relax	119			1					99.2
B=zero_contract		120							100.0
C=thirty_relax		1	118	1					98.3
D=thirty_contract				120					100.0
E=sixty_relax					120				100.0
F=sixty_contract						120			100.0
G=ninety_relax							120		100.0
H=ninety_contract								120	100.0

Precision (%)	100.0	99.2	100.0	98.4	100.0	100.0	100.0	100.0
---------------	-------	------	-------	------	-------	-------	-------	-------

#### 4.9 SUMMARY

Several analyses were done to evaluate the TD and FD features of anterior-posterior hand sides of HD-sEMG signals using classifiers. In sum, TD features (ARV and RMS) had higher correctly classified instances scores in classifying eight thumb attitudes compared to FD (MNF and MDF). Out of four classifiers used, LDA was selected as the best classifier for categorising the data. Also, the combination of hand sides (anterior-posterior) gave the highest correctly classified instances compared to the single-hand side. Then, the two highest correctly classified were further analysed. Details of the classification results using selected features, hand sides and classifier were further detailed using confusion matrixes.

## CHAPTER FIVE

### CONCLUSION AND RECOMMENDATIONS

#### 5.1 CONCLUSION

The research aims to investigate and establish the relationship between the synergy of the HD-sEMG signal from forearm musculature and thumb postures. Details of the accomplishments in achieving the research's objective are described in the sub-objectives as follows:

**5.1.1 To upgrade an existing portable thumb muscles platform and establish a standard sEMG recording setup for the HD-sEMG patch for consistent measurement of signals from the forearm musculature.**

To achieve the mentioned objective, an existing portable thumb muscle was upgraded to achieve the study design in fixing the thumb posture to be at zero degrees, thirty degrees, sixty degrees, and ninety degrees. Additionally, a trajectory interface was developed as a guide for the subjects during the data collection process to maintain the contract and relax conditions. A simple block diagram was used to develop the trajectory such as Analog input, Gain and Scope. The details were discussed in section 3.3. other than that, a standard sEMG recording setup was finalised and a standard patch placement for measuring EMG was set as the length of the forearm using the 25% rule. The details were elaborated extensively in section 3.4. Also, a portable biomedical signal amplifier called Sessantaquattro (manufactured by OT-Bioelettronica) was used in this research to capture

the HD-sEMG signals as elaborated in section 3.5. The force to be exerted by the subject was 30% MVC for contact condition and 0% for relax condition (at rest).

### **5.1.2 To Investigate The Signal For The Optimised Extraction Method And The Best Selection Of Features.**

Based on the literature (Huang et al., 2016; Khushaba et al., 2017; Siddiqi & Sidek, 2016), EMG signals can be differentiated using TD, FD, and a combination of time-and-frequency domain analyses. To achieve the objective, four features were extracted; two from TD analysis and another two from FD assessment. For the TD, the selected features were RMS and ARV, while MNF and MDF were used based on the evaluation of FD features. As TD features had higher accuracy than FD, these features were combined as ARV-RMS which was discussed in section 3.6.

### **5.1.3 To determine the best classifier and validate the performance of the developed system by classifying HD-sEMG data collected.**

There were four classifiers employed in this study, namely LDA, SVM, KNN, and TREE-based classifiers. The algorithms of each classifier were discussed in section 3.9. As elaborated in detail in Chapter 4, the outcome showed that the best classifier was LDA and the best domains were TD features (consisting of ARV and RMS) which had successfully classified the thumb attitudes with 91.1% accuracy. On the other hand, FD features achieved 72.7% accuracy. Importantly, the combination of features which was ARV-RMS with a combination of both hand side data (posterior-anterior) achieved 99.7% accuracy;

the same as the RMS feature's record. The result also has been validated using the trainlm training function with 3 hidden layers.

In conclusion, all sub-objectives were successfully achieved. It can be concluded that the LDA classifier obtained the highest average of correctly classified instances with 99.7% using a combination of RMS and ARV features for both anterior and posterior sides. Overall, relax conditions achieved higher correctly classified instances (99.9%) compared to contract conditions (99.6%). The average accuracy conditions (contract and relax) and attitudes (angle) for the ARV-RMS features were equal with a percentage accuracy of 99.75%. Meanwhile, the RMS feature scored 0.05% lower with a percentage of 99.7%. Even though the difference in accuracy between using ARV-RMS and RMS features seems small, it will contribute to a huge impact from the medical point of view in developing a prosthesis hand that can be replicated close to a normal hand.

## **5.2 LIMITATIONS AND RECOMMENDATIONS FOR FUTURE WORKS**

The limitation of the research that needs to be looked at for future improvements are described as follows:

### **5.2.1 Thumb Attitude**

Limitation: The thumb attitude used in this experiment focuses on thumb flexion. The attitude studied in this experiment does not cover all the thumb attitudes, namely abduction, adduction, opposition, and reposition. To create a perfect prosthesis hand, all the attitudes must be covered.

Recommendation: Modify the thumb attitude platform for other attitudes.

As the thumb attitudes in this experiment do not cover all the attitudes listed earlier, further modification of the current thumb attitude platform is suggested so that a wide range of thumb motions can be covered.

### **5.2.2 Hand Position or Posture**

Limitation: In this experiment, the position of the forearm was fixed to a neutral position only. As a note, there are still two different positions that can be included in the study, namely supination and pronation positions. These two positions are important to be considered on a hand for daily activities, sports activities such as playing badminton, and for working activities such as typing on a computer which requires the pronation position. Since every hand position will affect the position of the targeted muscles which directly influence the HD-sEMG reading, a new set of data can be collected to enrich the study results for further development of prosthetic hands for a smooth hand posture.



Recommendation: Increase the degree of freedom of the thumb attitude platform.

Besides developing a new thumb attitude platform, the current platform shall be modified by adding the degree of freedom for forearm positions.

### **5.2.3 Amputee Subjects**

Limitation: The findings of this study are limited to health subjects only as no amputee participants participated for data collection purposes.

Recommendation: Collect data from the amputee subjects.

The study design proposed in the experiment had successfully classified eight thumb attitudes. Even though the outcomes of the study are valid to be generalised as the EMG signals from healthy subjects are the same as amputee subjects (Asokan & Y.Saber, 2021), it would be interesting to compare the sEMG signals from both subjects in the future for diversity purposes to reduce the risk of accidentally having extreme or biased groups.

### **5.2.4 HD-sEMG Recording Device**

Limitation: The device used in the experiment was limited to collecting data on one forearm side at a time. As such, the time taken to collect the data for the anterior and the posterior side would be longer than collecting data simultaneously for both sides.

Recommendation: Explore other HD-sEMG signal recording devices

It is best to have a device that can record HD-sEMG signals from both hand sides at one time. Future work may explore other latest recording devices such as Quattrocento multichannel for time-saving. This simultaneous recording device may also offer better accuracy than the current device used (Sessantaquattro) and have four channels as the data collected were recorded at the same time, with the same thumb motions.

### **5.2.5 Dynamic Grip Transition**

**Limitation:** In this experiment, the thumb attitudes were fixed at zero-degree, thirty-degree, sixty-degree and ninety-degree angles only. Thus, the study on EMG signal during transition between different attitudes is still an open problem.

**Recommendation:** Dynamic grip transitions

It is recommended to add more thumb attitudes such as fifteen degrees (in between zero-degree and thirty-degree angles) in producing a smooth prosthetic arm in between the disposition of thumb movements. Other than fixing the thumb attitude, it would be more interesting to study dynamic grip transitions from one angle to another. Before transradial amputees can consider real-time active myoelectric control over a prosthetic thumb component in a device, more research is needed in this area.

### 5.3 PUBLICATION

One journal paper and one conference papers have been published as the part of thesis contribution:

**Muhammad Mukhlis Suhaimi**, Aimi Shazwani Ghazali, Ahmad Jazlan Haja Mohideen, and Shahrul Na'im Sidek, "Thumb Attitude Analysis using High Density Surface EMG: A Preliminary Survey" 2020 IEEE-EMBS Conference on Biomedical Engineering and Sciences (IECBES), Langkawi Island, Malaysia, 2021, DOI: 10.1109/IECBES48179.2021.9398767

**Muhammad Mukhlis Suhaimi**, Ahmad Jazlan Haja Mohideen, Aimi Shazwani Ghazali, and Shahrul Na'im Sidek, "Analysis of High-Density Surface Electromyogram (HD-sEMG) Signal for Thumb Posture Classification from Extrinsic Forearm Muscles" OAEN-Cogent Engineering, 2022, DOI: 10.1080/23311916.2022.2055445

One journal paper and one conference papers as to be published as the part of thesis contribution:

**Muhammad Mukhlis Suhaimi**, Aimi Shazwani Ghazali, Ahmad Jazlan Haja Mohideen, and Shahrul Na'im Sidek, "Explication of Extrinsic Forearm Muscles on the Classification of Thumb Position Using High-Density Surface Electromyogram." The International Journal of Integrated Engineering (IJIE)

Muhammad Hariz Hafizalshah, **Muhammad Mukhlis Suhaimi**, Aimi Shazwani Ghazali, Ahmad Jazlan, and Shahrul Na'im sidek "Analysis of Extrinsic Forearm Muscles using High-Density Surface Electromyogram (HD-sEMG) on Thumb Posture Classification." International Conference on Intelligent Systems Design and Engineering Applications (ISDEA 2022)

## REFERENCES

- Adewuyi, A. A., Hargrove, L. J., & Kuiken, T. A. (2016). An Analysis of Intrinsic and Extrinsic Hand Muscle EMG for Improved Pattern Recognition Control. *IEEE Transactions on Neural Systems and Rehabilitation Engineering*, 24(4), (pp.485–494). <https://doi.org/10.1109/TNSRE.2015.2424371>
- Alam, M. M., Khan, A. A., & Farooq, M. (2020). Effects of vibration therapy on neuromuscular efficiency & features of the EMG signal based on endurance test. *Journal of Bodywork and Movement Therapies*, 24(4), (pp. 325–335). <https://doi.org/10.1016/j.jbmt.2020.06.037>
- Alam, M. S., & Arefin, A. S. (2018). Real-Time Classification of Multi-Channel Forearm EMG to Recognize Hand Movements using Effective Feature Combination and LDA Classifier. *Bangladesh Journal of Medical Physics*, 10(1), (pp. 25–39). <https://doi.org/10.3329/bjmp.v10i1.39148>
- Aranceta-Garza, A. and Conway, B. A. (2019). Differentiating Variations in Thumb Position From Recordings of the Surface Electromyogram in Adults Performing Static Grips , a Proof of Concept Study. 7(May), (pp 1–11). <https://doi.org/10.3389/fbioe.2019.00123>
- Amma, C., Krings, T., & Jonas, B. (2015). *Advancing Muscle-Computer Interfaces with High-Density Electromyography*. 929–938.
- Arnold, E. M., Hamner, S. R., Seth, A., Millard, M., & Delp, S. L. (2013). How muscle fiber lengths and velocities affect muscle force generation as humans walk and run at different speeds. 216(11), 2150–2160. <https://doi.org/10.1242/jeb.075697>
- Asokan, A., & Y.Saber, A. (2021). Forearm Amputation. *StatPearls. Treasure Island (FL)*. <https://www.ncbi.nlm.nih.gov/books/NBK560932/>

- Bao, X., Zhou, Y., Wang, Y., Zhang, J., Lu, X., & Wang, Z. (2018). Electrode placement on the forearm for selective stimulation of finger extension / flexion. *61534003*, 1–22.
- Barru, S., Marque, P., & Duclay, J. (2018). Recurrent inhibition is higher in eccentric compared to isometric and concentric maximal voluntary contractions. *Acta Physiologica*, March. <https://doi.org/10.1111/apha.13064>
- Bashford, J., Wickham, A., Iniesta, R., Drakakis, E., Boutelle, M., Mills, K., & Shaw, C. E. (2020). Clinical Neurophysiology Preprocessing surface EMG data removes voluntary muscle activity and enhances SPiQE fasciculation analysis. *Clinical Neurophysiology*, 131(1), 265–273. <https://doi.org/10.1016/j.clinph.2019.09.015>
- Bi, Z., Wang, Y., Wang, H., Zhou, Y., Xie, C., Zhu, L., Wang, H., Wang, B., Huang, J., Lu, X., & Wang, Z. (2020). Wearable EMG Bridge - A Multiple-Gesture Reconstruction System Using Electrical Stimulation Controlled by the Volitional Surface Electromyogram of a Healthy Forearm. *IEEE Access*, 8, 137330–137341. <https://doi.org/10.1109/ACCESS.2020.3011710>
- Celadon, N., Došen, S., Binder, I., Ariano, P., & Farina, D. (2016). Proportional estimation of finger movements from high-density surface electromyography. *Journal of NeuroEngineering and Rehabilitation*, 13(1), (pp. 1–19). <https://doi.org/10.1186/s12984-016-0172-3>
- Chowdhury, R. H., Reaz, M. B. I., Ali, M. A. B. M., Bakar, A. A. A., Chellappan, K., & Chang, T. G. (2013). Surface Electromyography Signal Processing and Classification Techniques. *Pubmed* (pp. 12431–12466). <https://doi.org/10.3390/s130912431>
- Cordella, F., Ciancio, A. L., Sacchetti, R., Davalli, A., Cutti, A. G., Guglielmelli, E., & Zollo, L. (2016). Literature review on needs of upper limb prosthesis users. *Frontiers in Neuroscience*, 10(MAY), (pp. 1–14). <https://doi.org/10.3389/fnins.2016.00209>

- Dahlqvist, C., Nordander, C., Granqvist, L., Forsman, M., & Hansson, G. Å. (2018). Comparing two methods to record maximal voluntary contractions and different electrode positions in recordings of forearm extensor muscle activity: Refining risk assessments for work-related wrist disorders. *Work*, 59(2), 231–242. <https://doi.org/10.3233/WOR-172668>
- Dai, C., & Hu, X. (2019). Extracting and Classifying Spatial Muscle Activation Patterns in Forearm Flexor Muscles Using High-Density Electromyogram Recordings. *International Journal of Neural Systems*, 29(1). <https://doi.org/10.1142/S0129065718500259>
- Dupan, S. S. G., Stegeman, D. F., & Maas, H. (2018). Distinct neural control of intrinsic and extrinsic muscles of the hand during single finger pressing. *Human Movement Science*, 59(April), 223–233. <https://doi.org/10.1016/j.humov.2018.04.012>
- Enoka, R. M. (2019). Physiological validation of the decomposition of surface EMG signals. *Journal of Electromyography and Kinesiology*, 46(September 2018), 70–83. <https://doi.org/10.1016/j.jelekin.2019.03.010>
- Physiopedia. (n.d.). (2021), Extensor Pollicis Longus. [https://www.physiopedia.com/Extensor\\_Pollicis\\_Longus](https://www.physiopedia.com/Extensor_Pollicis_Longus)
- Frank, E., Hall, M., Holmes, G., Kirkby, R., & Witten, I. H. (2010). Data Mining and Knowledge Discovery Handbook. *Data Mining and Knowledge Discovery Handbook*, July, 0–10. <https://doi.org/10.1007/978-0-387-09823-4>
- Garcia, M. A. C., & Vieira, T. M. M. (2011). Surface electromyography: Why, when and how to use it. *Medicina Del Deporte*, 4(1), 17–28.
- Ghaderi, P., & Marateb, H. R. (2017). Muscle activity map reconstruction from high density surface EMG signals with missing channels using image inpainting and surface reconstruction methods. *IEEE Transactions on Biomedical Engineering*, 64(7), 1513–1523. <https://doi.org/10.1109/TBME.2016.2603463>

- Ghazali, A. S., Sidek, S. N., & Wok, S. (2015). Affective state classification using Bayesian classifier. *Proceedings - International Conference on Intelligent Systems, Modelling and Simulation, ISMS, 2015-Septe*, 154–158. <https://doi.org/10.1109/ISMS.2014.32>
- Goubault, E., Verdugo, F., Pelletier, J., Traube, C., Begon, M., & Dal Maso, F. (2021). Exhausting repetitive piano tasks lead to local forearm manifestation of muscle fatigue and negatively affect musical parameters. *Scientific Reports*, 11(1), 1–14. <https://doi.org/10.1038/s41598-021-87403-8>
- Hakonen, M., Piitulainen, H., & Visala, A. (2015). Current state of digital signal processing in myoelectric interfaces and related applications. *Biomedical Signal Processing and Control*, 18, 334–359. <https://doi.org/10.1016/j.bspc.2015.02.009>
- Higashi, S., Goto, D., Okada, S., Shiozawa, N., & Makikawa, M. (2019). Development of wearable EMG measurement system on forearm for wrist gestures discrimination. *2019 IEEE 1st Global Conference on Life Sciences and Technologies, LifeTech 2019*, 250–251. <https://doi.org/10.1109/LifeTech.2019.8884009>
- Huang, H., Li, T., Bruschini, C., Enz, C., Koch, V. M., Justiz, J., & Antfolk, C. (2016). EMG pattern recognition using decomposition techniques for constructing multiclass classifiers. *Proceedings of the IEEE RAS and EMBS International Conference on Biomedical Robotics and Biomechatronics, 2016-July*, 1296–1301. <https://doi.org/10.1109/BIOROB.2016.7523810>
- Inam, S., Harmain, S. Al, Shafique, S., Afzal, M., Rabail, A., Amin, F., & Waqar, M. (2021). A Brief Review of Strategies Used for EMG Signal Classification. *2021 International Conference on Artificial Intelligence, ICAI 2021*, 140–145. <https://doi.org/10.1109/ICAI52203.2021.9445257>
- Islam, M. J., Ahmad, S., Haque, F., Reaz, M. B. I., Bhuiyan, M. A. S., & Islam, M. R. (2022). Forearm Orientation and Muscle Force Invariant Feature Selection Method for Myoelectric Pattern Recognition. *IEEE Access*, 10, 1–1.

<https://doi.org/10.1109/ACCESS.2022.3170483>

- Jabir, S., Lyall, H., & Iwuagwu, F. C. (2013). The extensor pollicis brevis: a review of its anatomy and variations. *Eplasty*, 13, e35.
- Jordanic, M., Rojas-martínez, M., Mañanas, M. A., & Alonso, J. F. (2016). Spatial distribution of HD-EMG improves identification of task and force in patients with incomplete spinal cord injury. *Journal of NeuroEngineering and Rehabilitation*, 1–11. <https://doi.org/10.1186/s12984-016-0151-8>
- Jordanić, M., Rojas-Martínez, M., Mañanas, M. A., Alonso, J. F., & Marateb, H. R. (2017). A novel spatial feature for the identification of motor tasks using high-density electromyography. *Sensors (Switzerland)*, 17(7). <https://doi.org/10.3390/s17071597>
- Kanitz, G., Montagnani, F., Controzzi, M., Cipriani, C., & Member, S. (2018). Compliant Prosthetic Wrists Entail More Natural Use Than Stiff Wrists During Reaching , Not ( Necessarily ) During Manipulation. *IEEE Transactions on Neural Systems and Rehabilitation Engineering*, 26(7), 1407–1413. <https://doi.org/10.1109/TNSRE.2018.2847565>
- Kavya, S., Dhatri, M. P., Sushma, R., Krupa, B. N., Muktanidhi, S. D., & Kumar, B. G. (2016). Controlling the hand and forearm movements of an orthotic arm using surface EMG signals. *12th IEEE International Conference Electronics, Energy, Environment, Communication, Computer, Control: (E3-C3), INDICON 2015*, 1–6. <https://doi.org/10.1109/INDICON.2015.7443749>
- Khan, S. M., Khan, A. A., & Farooq, O. (2020). Selection of features and classifiers for EMG-EEG-Based upper limb assistive devices - A review. *IEEE Reviews in Biomedical Engineering*, 13, 248–260. <https://doi.org/10.1109/RBME.2019.2950897>



- Khushaba, R. N., Al-Timemy, A. H., Al-Ani, A., & Al-Jumaily, A. (2017). A Framework of Temporal-Spatial Descriptors-Based Feature Extraction for Improved Myoelectric Pattern Recognition. *IEEE Transactions on Neural Systems and Rehabilitation Engineering*, 25(10), 1821–1831. <https://doi.org/10.1109/TNSRE.2017.2687520>
- Li, X., Holobar, A., Gazzoni, M., Merletti, R., Rymer, W. Z., & Zhou, P. (2015). Examination of poststroke alteration in motor unit firing behavior using high-density surface EMG decomposition. *IEEE Transactions on Biomedical Engineering*, 62(5), 1242–1252. <https://doi.org/10.1109/TBME.2014.2368514>
- Maduri, P., & Akhondi, H. (2020). Upper Limb Amputation. (*StatPearls*). StatPearls Publishing, Treasure Island (FL). <https://www.ncbi.nlm.nih.gov/books/NBK540962/>
- OT Bioelettronica s.r.l (2020) Manual, U. (n.d.). *OTBioLab* +.
- Mastinu, E., Clemente, F., Sassu, P., Aszmann, O., Brånemark, R., Håkansson, B., Controzzi, M., Cipriani, C., & Ortiz-catalan, M. (2019). Grip control and motor coordination with implanted and surface electrodes while grasping with an osseointegrated prosthetic hand. *Journal of NeuroEngineering and Rehabilitation* 2, 1–10.
- Mohideen, A. J. H., & Sidek, S. N. (2011). Development of EMG circuit to study the relationship between flexor digitorum superficialis muscle activity and hand grip strength. *2011 4th International Conference on Mechatronics: Integrated Engineering for Industrial and Societal Development, ICOM'11 - Conference Proceedings*, May, 17–19. <https://doi.org/10.1109/ICOM.2011.5937200>
- Nait-ali, A., Biometric, W., & Meets, S. (2019). Towards High Density sEMG (HD-sEMG) Acquisition Approach for Biometrics Applications. In *Hidden Biometrics: When Biometric Security Meets Biomedical Engineering* (pp. 101–112). Springer Nature Singapore Pte Ltd.

- Physiopedia. (2021), Abductor pollicis longus. [https://www.physio-pedia.com/Abductor\\_pollicis\\_longus?utm\\_source=physiopedia&utm\\_medium=search&utm\\_campaign=ongoing\\_internal](https://www.physio-pedia.com/Abductor_pollicis_longus?utm_source=physiopedia&utm_medium=search&utm_campaign=ongoing_internal)
- Paul, Y., Goyal, V., & Jaswal, R. A. (2017). Comparative analysis between SVM & KNN classifier for EMG signal classification on elementary time domain features. *4th IEEE International Conference on Signal Processing, Computing and Control, ISPCC 2017, 2017-Janua*, 169–175. <https://doi.org/10.1109/ISPCC.2017.8269670>
- Phinyomark, A., Thongpanja, S., Quaine, F., & Laurillau, Y. (2013). *Optimal EMG Amplitude Detectors for Muscle- Computer Interface. Mci.*
- R. L. Drake, W. Vogl, A. W. M. Mitchell, R. Tibbitts, and P. R. (2015). Forearm Anterior Compartment And Hand. In *Gray's anatomy for students: flash cards* (3rd ed., pp. 233–253). Churchill Livingstone Elsevier.
- Rojas-martínez, M., Mañanas, M. A., & Alonso, J. F. (2012). High-density surface EMG maps from upper-arm and forearm muscles, *Journal of NeuroEngineering and Rehabilitation*. 1–17.
- Rozand, V., Cattagni, T., Theurel, J., Martin, A., & Lepers, R. (2014). Neuromuscular Fatigue Following Isometric Contractions with Similar Torque Time Integral. Pubmed 1–6.
- Sánchez-velasco, L. E., Arias-montiel, M., Guzmán-ramírez, E., & Lugo-gonzález, E. (2019). ScienceDirect A Low-Cost EMG-Controlled Anthropomorphic Robotic Hand for Power and Precision Grasp. *Sciencedirect* 1–17. <https://doi.org/10.1016/j.bbe.2019.10.002>
- Siddiqi, A. R., & Sidek, S. N. (2016). Estimation of continuous thumb angle and force using electromyogram classification. *International Journal of Advanced Robotic Systems*, 13(5), 1–12. <https://doi.org/10.1177/1729881416658179>

- Sidek, S. N., Roslan, M. R., Sidek, S., & Khalid, M. S. M. (2018). Thumb-tip force prediction based on hill's muscle model using electromyogram and ultrasound signal. *International Journal of Computational Intelligence Systems*, *11*(1), 238–247. <https://doi.org/10.2991/ijcis.11.1.18>
- Stegeman, D. F., Kleine, B. U., & Lapatki, B. G. (2012). High-density Surface EMG : Techniques and Applications at a Motor Unit Level. *Biocybernetics and Biomedical Engineering*, *32*(3), 3–27. [https://doi.org/10.1016/S0208-5216\(12\)70039-6](https://doi.org/10.1016/S0208-5216(12)70039-6)
- Toledo-Pérez, D. C., Rodríguez-Reséndiz, J., Gómez-Loenzo, R. A., & Jauregui-Correa, J. C. (2019). Support Vector Machine-based EMG signal classification techniques: A review. *Applied Sciences (Switzerland)*, *9*(20). <https://doi.org/10.3390/app9204402>
- Turgunov, A., Zohirov, K., Ganiyev, A., & Sharopova, B. (2020). Defining the Features of EMG Signals on the Forearm of the Hand Using SVM, RF, k-NN Classification Algorithms. *2020 Information Communication Technologies Conference, ICTC 2020*, 260–264. <https://doi.org/10.1109/ICTC49638.2020.9123287>
- Vieira, S., Lopez Pinaya, W. H., & Mechelli, A. (2019). Introduction to machine learning. In *Machine Learning: Methods and Applications to Brain Disorders*. Elsevier Inc. <https://doi.org/10.1016/B978-0-12-815739-8.00001-8>
- Wijk, U., & Carlsson, I. (2015). Forearm amputees' views of prosthesis use and sensory feedback. *Journal of Hand Therapy*, *28*(3), 269–278. <https://doi.org/10.1016/j.jht.2015.01.013>
- Wohlman, S. J., & Murray, W. M. (2013). Bridging the gap between cadaveric and in vivo experiments : A biomechanical model evaluating thumb-tip endpoint forces. *Journal of Biomechanics*, *46*(5), 1014–1020. <https://doi.org/10.1016/j.jbiomech.2012.10.044>
- Xu, W. F., Fang, Y. F., Zhang, G. Y., Ju, Z. J., Li, G. F., & Liu, H. H. (2018). Surface Emg Channel Selection for Thumb Motion Classificationsignal. *Proceedings - International Conference on Machine Learning and Cybernetics*, *2*, 662–666.

<https://doi.org/10.1109/ICMLC.2018.8526988>

Yan, L., et al. (2019). Thumb Amputations Treated With Osseointegrated Percutaneous Prostheses With Up to 25 Years of Follow-up. *Wolters Kluwer Health American Academy of Orthopaedic Surgeons*. <https://doi.org/10.5435/JAAOSGlobal-D-18-00097>

Yu, Y., Sheng, X., Guo, W., & Zhu, X. (2018). Attenuating the impact of limb position on surface EMG pattern recognition using a mixed-LDA classifier. *2017 IEEE International Conference on Robotics and Biomimetics, ROBIO 2017, 2018-Janua*, 1497–1502. <https://doi.org/10.1109/ROBIO.2017.8324629>

Ziegler-graham, K., Mackenzie, E. J., Ephraim, P. L., Travison, T. G., Brookmeyer, R., K, A. Z., & Ej, M. (2008). *Estimating the Prevalence of Limb Loss in the United States : 2005 to 2050*. 89(March), 422–429. <https://doi.org/10.1016/j.apmr.2007.11.005>

# APPENDIX I: IREC APPROVAL



RESEARCH MANAGEMENT CENTRE

Our Ref. : IIUM/504/14/11/2/ IREC 2020-080  
Date : 29 July 2020

Asst. Prof. Dr. Aimi Shazwani binti Ghazali (Principal Investigator)  
Kulliyah of Engineering  
IIUM Gombak Campus  
53100 Gombak

Dear Asst. Prof. Dr.,

The IIUM Research Ethics Committee (IREC) has reviewed your study protocol as mentioned below:-

ID NO. : IREC 2020-080  
TITLE : Study of Thumb Attitude Relationship to Extrinsic Musculature Characterizations using High Density Surface Electromyogram Signals  
REGISTRATION DATE : 21 Jun 2020  
CO- INVESTIGATOR : Asst. Prof. Dr. Ahmad Jazlan Bin Haja Mohideen  
STUDENT : Muhammad Mukhlis bin Suhaimi (Postgraduate Student)  
STUDY SITE : IIUM Gombak  
SAMPLE SIZE : 40  
ETHICAL EXPIRY DATE : 21 July 2021

The IIUM Research Ethics Committee (IREC) operates in accordance to the Declaration of Helsinki, International Conference of Harmonization Good Clinical Practice Guidelines (ICH-GCP), Malaysia Good Clinical Practice Guidelines and Council for International Organizations of Medical Sciences (CIOMS) International Ethical Guidelines

The following documents have been received and reviewed to the above study:-

1. Study Proposal/Protocol: Version 1, dated 19 Jun 2020
2. Informed Consent Form (ICF) –
  - i. Information Sheet (English) – Version 1, dated 19 Jun 2020
  - ii. Consent Form (English) – Version 1, dated 19 Jun 2020
3. Questionnaire - Version 1, dated 19 Jun 2020
4. Approval Letter from Kulliyah of Engineering, IIUM
5. Principal Investigator's CV



*Garden of Knowledge and Virtue*

Office Address: Research Management Centre, Level 1, Block 2, Office of The Campus Director, IIUM Kuantan Campus,  
Jalan Sultan Ahmad Shah, Bandar Indera Mahkota, 25200 Kuantan Pahang.  
Tel: +609 570 4220 / 4223 Fax: +609 571 6741 E-mail: rmckuantan@iium.edu.my Website: www.iium.edu.my/research

Decision by IIUM Research Ethics Committee (IREC):

(√) Approved  
( ) Disapproved

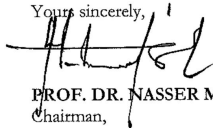
Date of Approval: 21 July 2020

The investigator(s) are required to:

- a) submit the 'Continuing Review Form' 30 days before EXPIRY DATE to renew Ethical Approval.
- b) notify IREC of any change in protocol and obtaining further ethical approval as appropriate.
- c) report any adverse incident during the course of a study to IREC even if the incident is not directly related to the study.
- d) report to the IREC within 72 hours for all internal SAEs (occurring in IIUM PI site).
- e) report in a prompt manner if the information impacts the continued ethical acceptability of the trial for external SAEs (occurring in participants at other sites).
- f) provide information of minor protocol deviation in Progress Report or End Report whichever necessary.
- g) report any major protocol deviation occurs within 5 working days.
- h) submit Progress Report Form before the end of six (6) month given by IREC.
- i) complete and submit the End of Project Report Form to the IREC Secretariat's Office.
- j) All records and data subjects are **CONFIDENTIAL** and used only for the purposes of this study and all issues and procedures on data confidentiality must be observed.

Thank you.

Yours sincerely,



**PROF. DR. NASSER MUHAMMAD AMJAD**  
Chairman,  
IIUM Research Ethics Committee (IREC)

Copy : File -IREC 2020-080

DISCLAIMER: The approval letter only covers the ethical aspect of your study only. Any other permission/approval to use any facilities, data or human resource should fall under applicant's responsibility.

## APPENDIX II: CONSENT FORM

Version: 1  
Date: 19-6-20



### [Informed Consent Form for Healthy Subject]

This informed consent form is for healthy subject.

**Name of Principle Investigator:** Dr. Aimi Shazwani Binti Ghazali

**Name of Organization:** Department of Mechatronics Engineering, International Islamic University Malaysia

**Name of Project and Version:** Study of Thumb Attitude Relationship to Extrinsic Musculature Characterizations using High Density Surface Electromyogram Signals

**This Informed Consent Form has two parts:**

- Information Sheet (to share information about the study with you)
- Certificate of Consent (for signatures if you choose to participate)

**You will be given a copy of the full Informed Consent Form**

## **PART I: INFORMATION SHEET**

### **Introduction**

I am Dr. Aimi Shazwani binti Ghazali, a lecturer at Kuliyyah of Engineering, International Islamic University Malaysia (IIUM). Hereby, my research assistant, Br. Mukhlis and I would like to invite you to participate in a study related to thumb activities.

This study will be conducted at Biomechanics Research Laboratory, IIUM. You will be asked to attend only one session which may last approximately 1 hours (including several short breaks in between the experimental sessions).

### **Purpose**

Clinically, the attitude of the thumb controls by the intrinsic muscles located at palm. However, the extrinsic muscles located at forearm has information that governing the thumb attitude. The information at the forearm muscles that indirectly governing the thumb attitude can be extract and be uses in developing an advance hand prosthesis. We believe that you can help us by participating in this research. The aim of this research is to study the pattern of active muscle on the forearm during different thumb attitude.

### **Participant selection**

We are asking you to consider participating in this study because you do not suffer from any systematic inflammatory, connective tissue disorders, or other medical disorders, and you are not pregnant. We are inviting a total of 30 people.

### **Voluntary Participation**

You can choose to say no and any services that you and your family receive at this centre will not change. You can ask as many questions as you like and we will take the time to answer them. You don't have to decide today. You can think about it and tell us your decision later.

### **Procedure**

A. Once you have decided to take part in this research, our research team will discuss the study with you and answer any questions you may have. If you are still happy to take part, we will ask you to sign the consent form.

You will be asked to attend one session, lasting approximately 1 hours. We need to prepare the experiment for about 10 minutes, and you can have a rest between the experiment sessions.

B. We will ask you to provide us with some information regarding your age, sex, dominant hand, height, and any history of foot, leg or pelvis pain or injury. The information recorded is confidential, your name is not being included on the forms, only a number will identify you, and no one else except the researchers.

You will be asked to sit upright with the hand will put at the experiment platform. To collect the activity of your muscles, High Density surface EMG will then be attached on the on the skin of forearm for both side anterior and posterior. You will be asked to push the knob or pressure sensor on the platform. The position or angle of the knob will be changed accordingly for each activity.



There will be eight tests with different positions or angle of the knob for both side of electrode placement, where:

- Test 1: knob at 90° and extract data at anterior side
- Test 2: knob at 90° and extract data at posterior side
- Test 3: knob at 60° and extract data at anterior side
- Test 4: knob at 60° and extract data at posterior side
- Test 5: knob at 30° and extract data at anterior side
- Test 6: knob at 30° and extract data at posterior side
- Test 7: knob at 0° and extract data at anterior side
- Test 8: knob at 0° and extract data at posterior side

**Duration**

Time for a session to complete will take about 1 hours and 15 minutes per participant.

**Risks and Discomforts**

The adhesive used to attach the electrodes to your skin may cause some redness. If you have any allergies or skin conditions (e.g. eczema, dermatitis, etc.), please inform the researchers prior to the placement of the electrodes, as you may be unable to take part. If you notice any irritation during or immediately following the study, please inform the researcher.

If you experience any muscle or joint pain and/or discomfort during the session please inform the researcher, and if you need to rest and/or want to stop, you can do so at any time.

**Benefits**

The information collected from your thumb muscle activities will assist us in understanding and analysing the pattern activation muscles for different thumb attitudes. This study is significant in the development of hand prosthesis for those who lost.

**Reimbursements**

You will be granted with a token of appreciation for the time and effort you spent for this study.

**Confidentiality:**

We will not be sharing personal information about you to anyone outside of the research team.

Neither your name nor any other identifying information will be associated with this study. It will be completely anonymous and it cannot be traced back to you. Neither your name nor any other identifying information (such as your voice or picture) will be used in presentations or in written products resulting from the study without your written consent.

**Sharing of Research Findings**

Only the research team will be able to view the material and the data collected from you will be used only for scientific analysis. Also, the information that we collect from this study also will be used for writing scientific publications and will only be reported at group level. No individual subject will be identified in any report or presentation arising from the research.

Unfortunately, we are unable to provide you with your individual results; however, you can be provided with a summary report of our findings at the end of the study, upon your request.

**Right to refuse or withdraw**

You do not have to take part in this research if you do not wish to do so, and choosing to participate will not affect your job or job-related evaluations in any way. You may stop participating in the experiment at any time that you wish without your job being affected. I will give you an opportunity at the end of the experiment to review your remarks, and you can ask to modify or remove portions of those, if you do not agree with my notes or if I did not understand you correctly.

**Who to Contact**

If you have any questions you may ask them now or later, even after the study has started. If you wish to ask questions later, you may contact:

***Dr. Aimi Shazwani Binti Ghazali***  
***Phone: 013-2229406***  
***aimighazali@iium.edu.my***

***Mohammad Mukhlis bin Suhaimi***  
***Phone: 010-5778585***  
***ibnusuhaimi94@gmail.com***

This proposal has been reviewed and approved by IIUM Research Ethics committee (IREC), which is a committee whose task it is to make sure that research participants are protected from harm. If you wish to find about more about the IREC, you may visit to this web <http://iium.edu.my/irec>

You can ask me any more questions about any part of the research study if you wish to. Do you have any questions?

**PART II: CERTIFICATE OF CONSENT**

**Certificate of Consent**

I have read the foregoing information related to this study in extracting EMG reading at my forearm using HD-sEMG with 64 electrode arranged 13-by-5. I have been given the opportunity to ask questions about the study and all of the questions have been answered to my satisfaction. I consent voluntarily to participate in this study.

**Name of Participant:** \_\_\_\_\_

**Identity Card (IC) / Passport Number:** \_\_\_\_\_

**Signature of Participant:** \_\_\_\_\_

**Date:** \_\_\_\_\_  
**Day/month/year**

I witness the accurate reading of the consent form by the potential participant, and the participant has been given the opportunity to ask questions. I confirm that the participant has given his/her consent freely.

**Name of witness** \_\_\_\_\_

**Identity Card (IC) / Passport Number :** \_\_\_\_\_

**Signature of witness** \_\_\_\_\_

**Date:** \_\_\_\_\_  
**Day/month/year**

**Statement by the researcher/person taking consent**

I have accurately read out the information sheet to the potential participant, and to the best of my ability made sure that the participant understands the research procedures.

I confirm that the participant was given an opportunity to ask questions about the study, and all the questions asked by the participant have been answered correctly and to the best of my ability. I confirm that the individual has not been coerced into giving consent, and the consent has been given freely and voluntarily.

A copy of this ICF has been provided to the participant.

**Researcher(s)**

1. Dr. Aimi Shazwani Binti Ghazali
2. Muhammad Mukhlis bin Suhaimi

Signature:  
Date:

Signature:  
Date: